ELSEVIER

Palaeogeography, Palaeoclimatology, Palaeoecology 191 (2003) 269–300

PALAEO

www.elsevier.com/locate/palaeo

Permian climatic and paleogeographic changes in Northern Gondwana: the Khuff Formation of Interior Oman

L. Angiolini [a,*], M. Balini [a], E. Garzanti [b], A. Nicora [a], A. Tintori [a], S. Crasquin [c], G. Muttoni [a]

[a] *Dipartimento di Scienze della Terra, Via Mangiagalli 34, 20133 Milan, Italy*
[b] *Dipartimento di Scienze Geologiche e Geotecnologiche, Piazza della Scienza 4, 20126 Milan, Italy*
[c] *CNRS – FRE 2400, Université Pierre et Marie Curie, Département de Géologie Sédimentaire, case 104, 75252 Paris Cedex 05, France*

Received 15 October 2001; accepted 18 November 2002

Abstract

Detailed stratigraphic, paleontologic, and petrographic data from the Middle Permian Khuff Formation exposed in the Haushi–Huqf area of Interior Oman provide new insight into the Permian climatic evolution of the northern Gondwana margin, and on the still debated timing of Neotethys opening between Gondwana and the Cimmerian blocks. The Khuff Formation is interpreted to record a major transgression of Neotethyan waters in Wordian times (Middle Permian), at a stage of full oceanization and tectonic quiescence, when thermal subsidence caused final drowning of rift shoulders and deposition of marine carbonates onto vast portions of stable Arabia. The petrographic composition of Middle Permian sandstones indicates a post-rift stage, and documents a long-term increase in mineralogic stability ascribed to a shift toward warm–humid climatic conditions, coupled with reduced relief and longer transit times of detritus from source to basin. Raising temperatures and northward latitudinal drift towards lower tropic latitudes throughout the Permian are fully documented by rich transitional marine faunas and available paleomagnetic evidence.

Keywords: Neotethys opening; Guadalupian transgression; paleontology; biostratigraphy; sandstone petrography; chemical weathering

1. Introduction

The Permian succession of the Haushi–Huqf area (Interior Oman) at the northern Gondwana margin contains valuable paleogeographic and paleoenvironmental information during a crucial time for Earth life, culminating at the end of the period with a dramatic multicausal mass extinction which profoundly altered the course of evolution.

The principal aim of this work is to constrain, through integrated paleontologic, sedimentologic,

* Corresponding author.
E-mail address: lucia.angiolini@unimi.it (L. Angiolini).

0031-0182/02/$ – see front matter © 2002 Elsevier Science B.V. All rights reserved.
doi:10.1016/S0031-0182(02)00668-5

and petrographic analysis, the paleoclimatic and paleogeographic evolution of Oman as part of the northern Gondwana margin at mid-Permian times. Unraveling the climatic evolution of Northern Gondwana, from glacial conditions in the earliest Permian to tropic climates in the Middle Permian, is crucial to the understanding of the dynamics of paleogeographic and environmental change at the close of the Paleozoic.

Precise timing of break-up and detachment of the Cimmerian blocks from Gondwana is still debated. According to most authors, Neotethyan rifting took place in the Early Permian, leading to initial opening in the Middle Permian (e.g. Bechennec et al., 1990; Blendinger et al., 1990; Stampfli et al., 1991; Pillevuit, 1993; Le Métour et al., 1994; Glennie, 2000).

However, stratigraphic and petrographic data from the Himalayan arm of Neotethys indicate that rifting began as early as the Early Carboniferous (Vannay, 1993; Garzanti et al., 1996a; Garzanti and Sciunnach, 1997), whereas break-up occurred at late Sakmarian times (Garzanti et al., 1994, 1996b, 1999). An east to west diachronous opening of Neotethys, starting north of Australia in the Carboniferous, has been proposed by Stampfli (2000).

Recent sedimentologic, biostratigraphic, and petrographic work in Interior Oman has shown that the failed Madagascar arm of Neotethys also experienced extension in the Carboniferous (Al-Belushi et al., 1996), with tectonic climax and unroofing of Pan-African basement granitoids occurring prior to the late Sakmarian transgression (Angiolini et al., in press). Furthermore, marine bioprovinciality changes along the Peri-Gondwanan fringe indicate that the main Neotethys arm should have opened before the Middle Permian (Angiolini, 2001). On this basis, the main Neotethys, Himalayan and Madagascar arms were interpreted as the three arms of a rift–rift–rift triple junction, situated just off the northeast corner of Oman, between the future Arabian and India plates and the Cimmerian continents (Central Iran, Central Afghanistan, Karakorum, Lhasa) (Al-Belushi et al., 1996; Angiolini et al., in press).

This paper presents a detailed stratigraphic, paleontologic and petrographic synthesis of the Khuff Formation of Interior Oman, and briefly discusses its correlation with the Saiq Formation of the Oman Mountains, focusing on two major topics:

(1) the Wordian transgression in relation to the onset of thermal subsidence of the newly formed North Oman margin, as caused by fast spreading along the main Neotethys arm;

(2) the marked climatic warming and rise of humidity through the Early to Middle Permian.

The Khuff Formation and the underlying Gharif Formation represent a key succession for the intercalibration of Middle Permian marine and continental biostratigraphic scales. On the one hand, a very significant paleoflora (Broutin et al., 1995) occurs together with a rich and diversified marine fauna; on the other hand, the biota shows a marked transitional character, being represented by wide-ranging, Gondwanan, paleoequatorial and endemic Cimmerian taxa, allowing correlation among different biogeographic realms. The Permian succession of the Arabian subcontinent is known to be crucial for hydrocarbon exploration, the Khuff Formation in particular being one of the major regional seals of the Oman Salt Basin, capping several sandy reservoirs within the underlying Gharif Formation.

This synthesis is based on paleontologic, sedimentologic and petrographic analyses in the Haushi–Huqf area of Interior Oman (Fig. 1), carried out during several geologic surveys from 1995 to 2001 by the Università degli Studi of Milan and Université Pierre et Marie Curie of Paris VI, with the lead and help of BRGM geologists J.P. Platel (Bordeaux) and J. Roger (Orleans), in the framework of the Peri-Tethys Program and Italian CNR and COFIN projects.

2. Geological setting

The Sultanate of Oman forms the easternmost part of the Arabian subcontinent, delimited by the Neogene to Late Mesozoic oceanic crust of the Gulf of Aden, Owen Basin, and Gulf of Oman. The studied area is located in eastern Interior Oman, where the autochthonous sedimentary

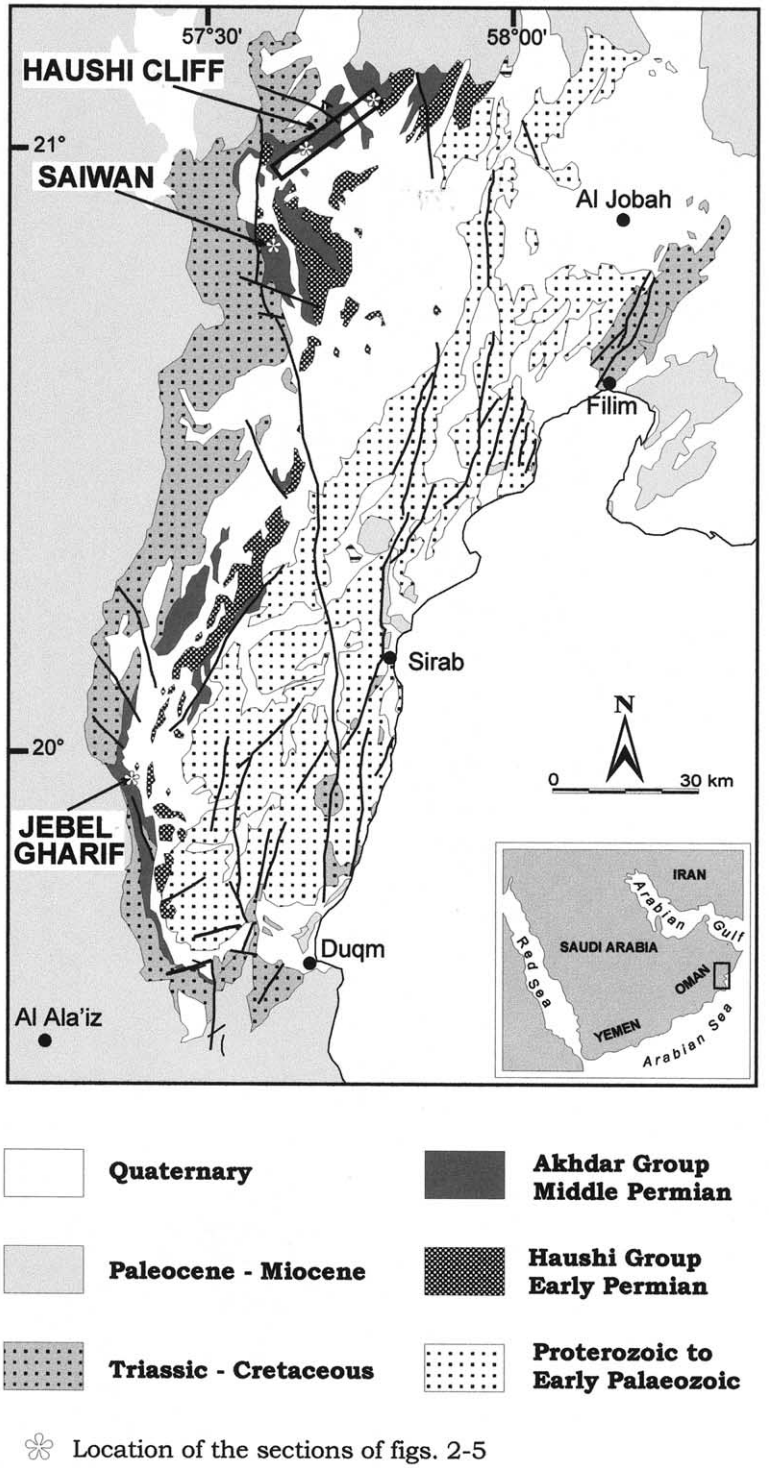

Fig. 1. Geologic sketch map of the Haushi–Huqf. Modified from Bechennec et al. (1993).

cover of the Arabian shield crops out in the broad Haushi–Huqf arch (Fig. 1). This area, of long-standing interest to oil geologists, corresponds to a polyphase anticlinal structure cored by Upper Proterozoic strata, with only a very small exposure of Pan-African igneous rocks at its northern edge.

The Lower to Middle Permian succession of the Haushi–Huqf consists of two major sequences, including several unconformities. The first sequence (Haushi Group), disconformably overlying Upper Proterozoic–Lower Paleozoic units, comprises Lower Permian glacio-lacustrine, glacio-fluvial, alluvial and paralic deposits of the Al Khlata Formation (Levell et al., 1988; Al-Belushi et al., 1996), unconformably transgressed by marine sandy calcarenites of the Saiwan Formation (Dubreuilh et al., 1992; Roger et al., 1992). The sharp base of the Saiwan Formation, dated biostratigraphically as early Sterlitamakian (late Sakmarian), records a major transgression related to final deglaciation and consequent global sea-level rise, as indicated by ravinement surfaces associated with lag deposits with tree trunks, reworked ferruginous pedogenic concretions and phosphate, and by paleoecologic analyses (Angiolini et al., in press). This unconformity is also interpreted, on both biogeographic and petrographic grounds, to correspond with initial sea-floor spreading in the Neotethys Ocean (Angiolini et al., in press).

The second sequence (Akhdar Group), resting unconformably on the Haushi Group, spans the ?Artinskian to Wordian time interval (Broutin et al., 1995; Angiolini et al., 1998). It includes the fluvial to tidal sandstones and mudrocks of the Gharif Formation, indicating main sediment transport towards the west to northwest (Crumeyrolle et al., 1997), conformably overlain by marine marlstones and bioclastic limestones of the Khuff Formation. In the Haushi area, the Khuff Formation is disconformably capped by a thin horizon of plant-bearing continental red-beds and laterite/bauxite paleosols (Minjur Formation), spanning the Triassic to Early Jurassic. In Jabal Gharif, the Lower Cretaceous Jurf and Qishn formations directly lap onto the Khuff Formation.

The Khuff Formation is biostratigraphically correlated with the lower part of the Saiq Formation cropping out in the northwestern Jabal Akhdar window (Oman Mountains). The Saiq Formation, lying with spectacular angular unconformity on the Proterozoic series of the Arabian Platform and including basal conglomerates, bioclastic limestones and coral boundstones capped by dolostones, marks the final transgression on the Neotethyan rift shoulder.

3. The Khuff Formation

The Khuff Formation was formally introduced by Steineke et al. (1958) to comprise Middle–Upper Permian carbonate rocks of Central Arabia. Syntheses of the Khuff Formation of south–central Saudi Arabia have recently been published by Al-Aswad (1997) and Sharland et al. (2001).

The best outcrops of the Khuff Formation in Oman are represented by a number of sections, located east of Wadi Lusaba, between 21°00′34″N 57°39′35″E and 21°02′09″N 57°42′22″E, along the northwestern flank of the Haushi uplift (Figs. 1–3). The Khuff Formation has also been measured: (1) in the Saiwan area (short log located at 20°51′43″N 57°36′10″E) (Figs. 1 and 4); and (2) at Jabal Gharif (section starting at 19°57′01″N 57°21′38″E) (Figs. 1 and 5).

3.1. Lithology

In the Haushi area, the Khuff Formation conformably overlies the cross-laminated to bioturbated sandstones of the uppermost Gharif Formation. The Khuff Formation reaches a maximum thickness of 30–40 m, and consists of white to gray marls and bioclastic limestones rich in brachiopods, conodonts, foraminifers, algae, ammonoids, nautiloids, trilobites, gastropods, bivalves, scaphopodes, ostracodes, crinoids, corals, bryozoans, and fish remains. White to yellow and light gray sandstones are common in the lower part of the unit; wave-rippled sandy limestones occur intercalated in the upper part.

Dubreuilh et al. (1992), Broutin et al. (1995) and Angiolini et al. (1998) placed the base of the formation at the first occurrence of marine

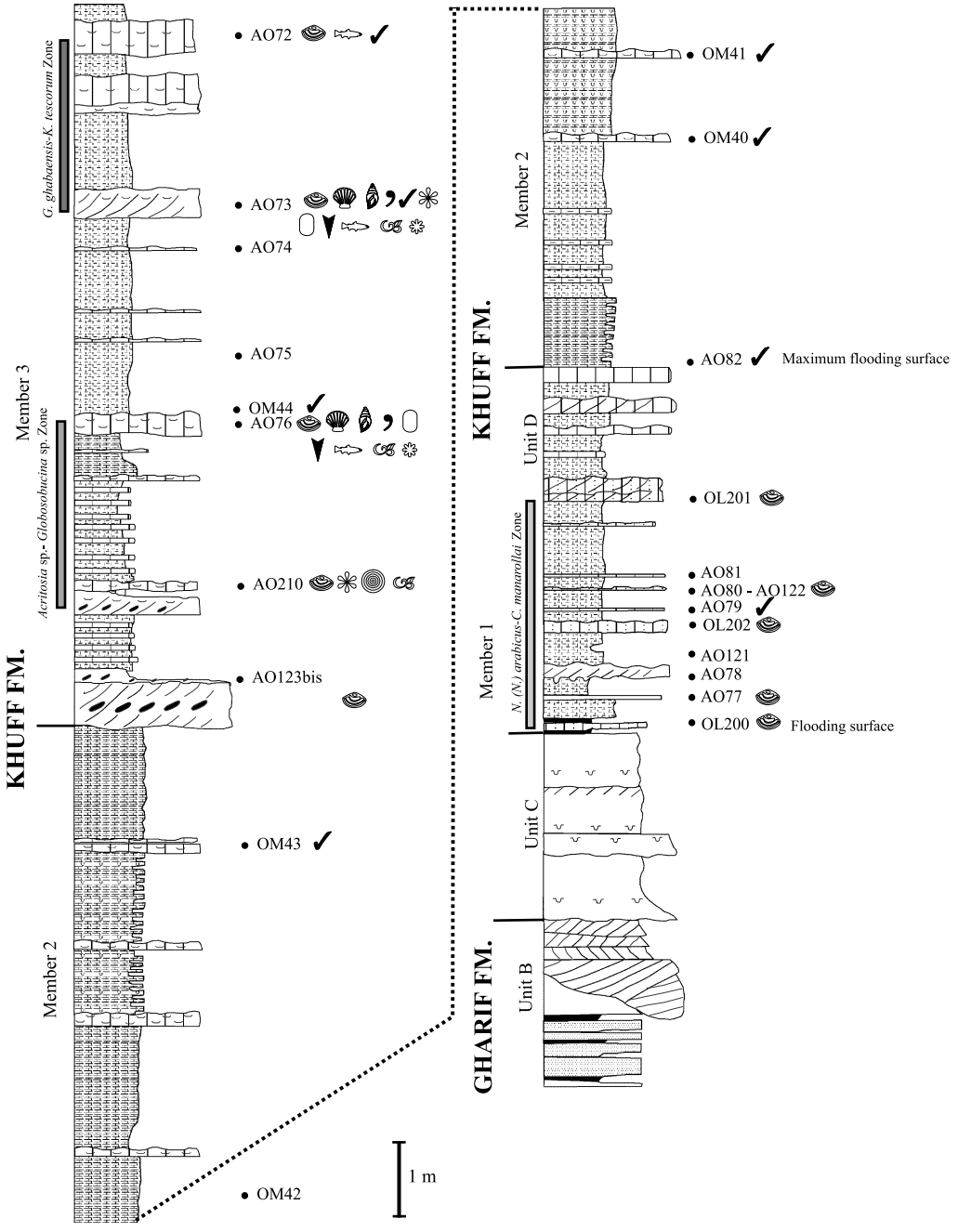

Fig. 2. Stratigraphic section K7 of the Khuff Formation in the Haushi area, starting at 21°00′35″N 57°39′27″E. The extension of three brachiopod assemblage biozones is reported on the left hand side of the column. It is one of the thickest sections in the area and it is cut northward by the ?Triassic–Jurassic Minjur Formation. Legend as in Fig. 3.

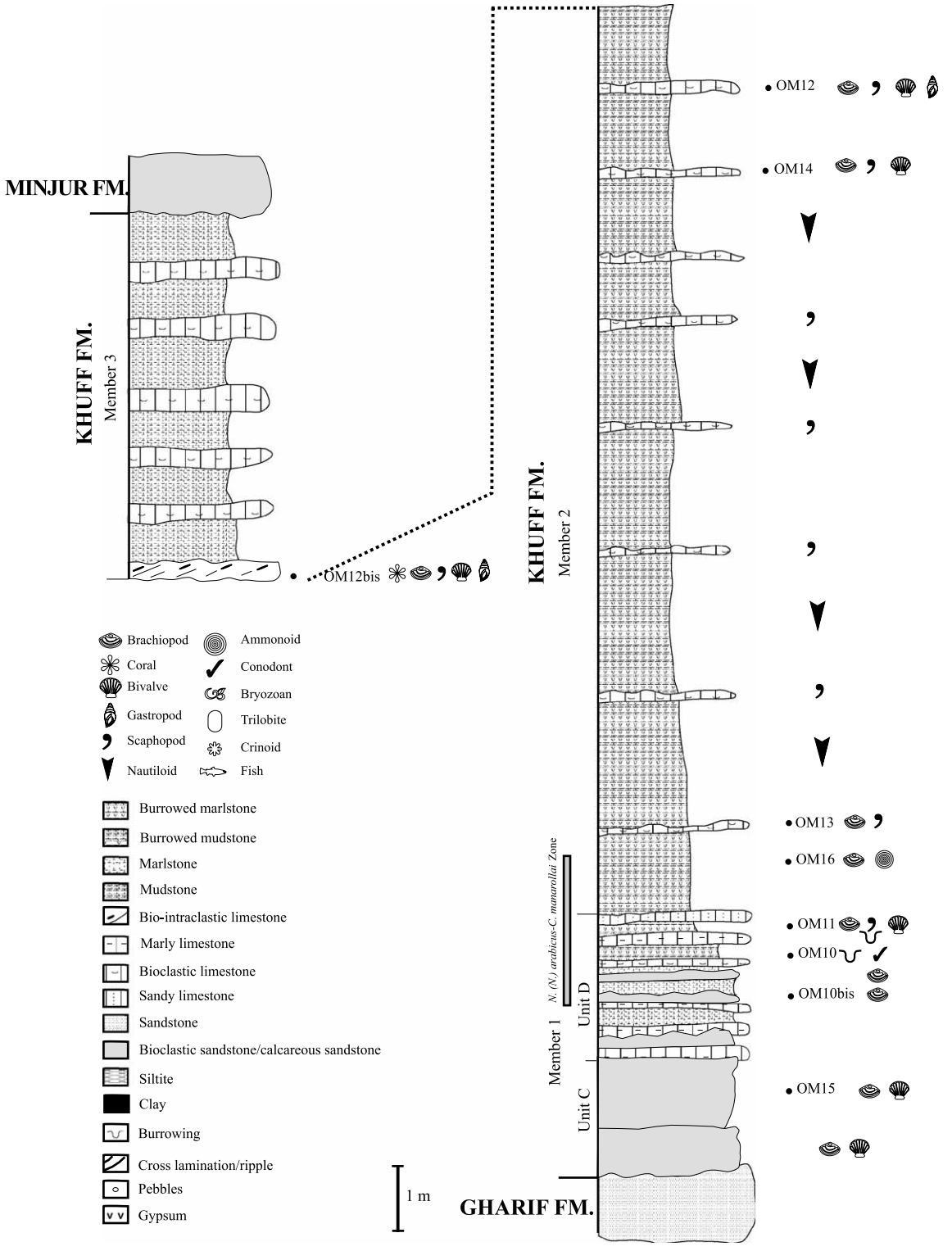
MINJUR FM.
KHUFF FM.
Member 3
OM12bis
KHUFF FM.
Member 2
OM12
OM14
OM13
OM16
OM11
OM10
OM10bis
OM15
N. (N.) arabicus-C. manarollai Zone
Member 1
Unit D
Unit C
GHARIF FM.
1 m
Brachiopod
Coral
Bivalve
Gastropod
Scaphopod
Nautiloid
Ammonoid
Conodont
Bryozoan
Trilobite
Crinoid
Fish
Burrowed marlstone
Burrowed mudstone
Marlstone
Mudstone
Bio-intraclastic limestone
Marly limestone
Bioclastic limestone
Sandy limestone
Sandstone
Bioclastic sandstone/calcareous sandstone
Siltite
Clay
Burrowing
Cross lamination/ripple
Pebbles
Gypsum

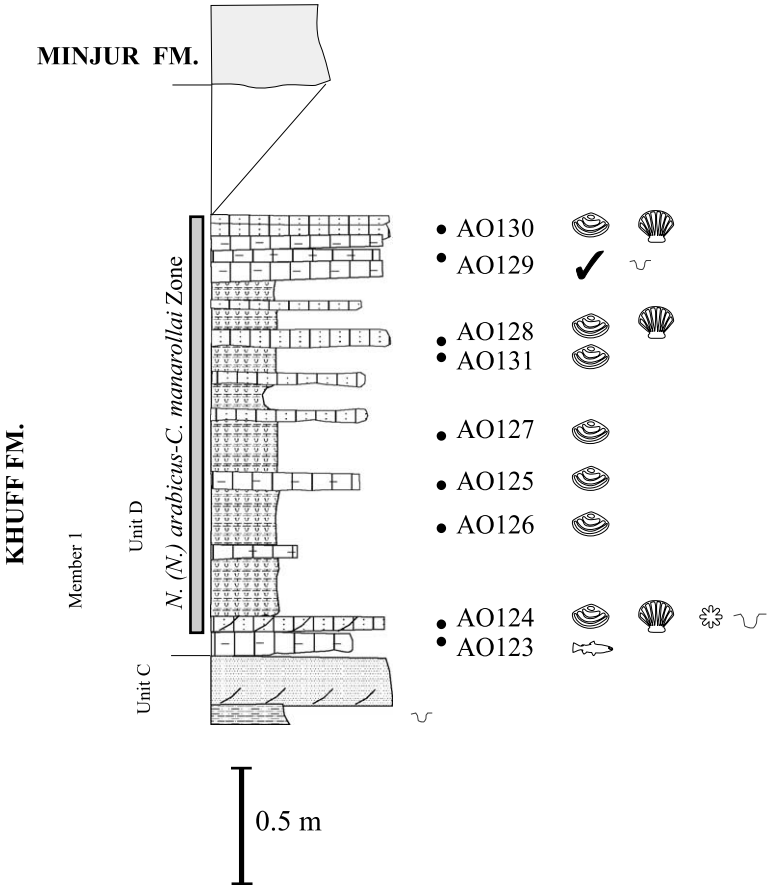

Fig. 4. Stratigraphic section of the Khuff Formation at Saiwan, starting at 20°51′43″N 57°36′10″E. Only Member 1 of the Khuff Formation crops out below the basal Minjur unconformity. Legend as in Fig. 3.

bioclasts in the basal clastic rocks (boundary between units B and C in Fig. 2). Marine influence, however, is also recorded by tidal sandstones below this boundary (unit B).

The top of the Khuff Formation is unconformably truncated by paleosols of the Minjur Formation. This regional angular unconformity cuts across the Khuff Formation down to its basal member in the Saiwan area (Fig. 4). The unit gradually pinches out south of the Jabal Gharif area, where the Lower Cretaceous Thamama Group laps directly onto the Gharif Formation.

The Khuff Formation has been subdivided into three members (Figs. 2–5). Member 1 comprises two different lithozones. The lower lithozone (unit C) is characterized by cross-bedded, bioclastic pebbly sandstones displaying herringbone to polymodal cross-lamination, and containing highly abraded marine bioclasts and mud intraclasts up to 5 cm in diameter. The upper lithozone (unit D), sharply overlying unit C, is characterized by bioclastic limestones interbedded with marlstones. Thin to medium sandstone beds with NNE/SSW-directed straight-crested wave ripples are intercalated at the base, and progressively disappear upward. The upper lithozone shows cyclo-

Fig. 3. Stratigraphic section I1 of the Khuff Formation in the Haushi area, starting at 21°02′09″N 57°42′22″E. Brachiopod taxa above the *Neochonetes* (*Nongtaia*) *arabicus–Celebetes manarollai* Biozone do not allow identification of the overlying biozones.

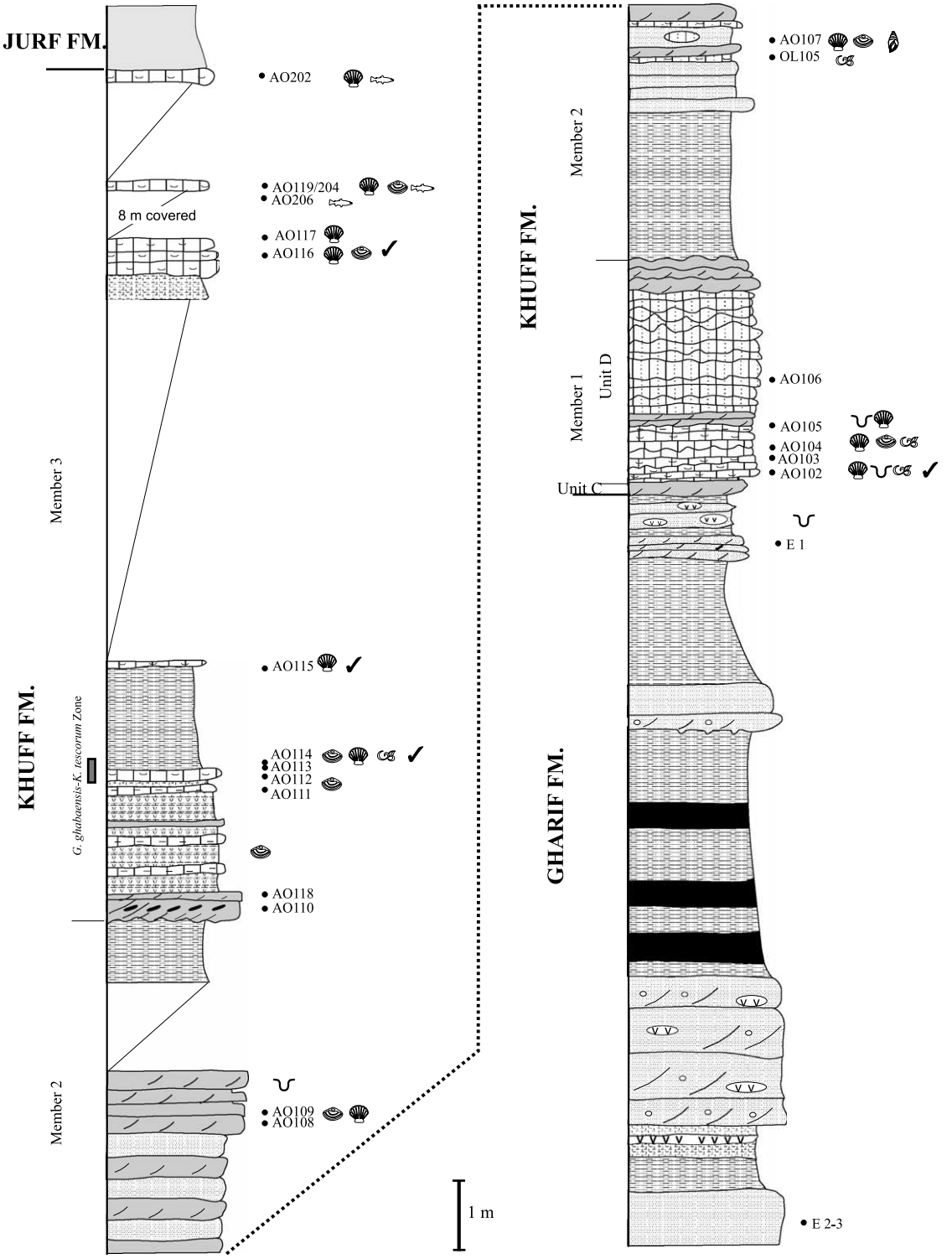
JURF FM.
AO202
AO119/204
AO206
8 m covered
AO117
AO116
Member 3
KHUFF FM.
G. ghabaensis-K. tescorum Zone
AO115
AO114
AO113
AO112
AO111
AO118
AO110
Member 2
AO109
AO108
1 m
KHUFF FM.
Member 2
AO107
OL105
Member 1
Unit D
AO106
AO105
AO104
AO103
AO102
Unit C
E 1
GHARIF FM.
E 2-3

thems consisting of wave-reworked, lower shoreface sandstones. It passes upward, with sharp flooding surface encrusted by bryozoans, to inner-shelf bioclastic limestones with sparse isolated wave ripples and *Ophiomorpha* burrows. Next, conodont-bearing outer-shelf marlstones with *Zoophycos*-type burrows are finally overlain by shallower-water bioclastic sandy marls with truncated wave ripples.

Member 2 consists of outer-shelf burrowed marlstones and marly limestones, rhythmically interbedded with thin sandy bioclastic layers with sharp flat base. It overlies rather sharply Member 1, whereas transition to Member 3 is gradual, with progressive increase of coarser-grained bioclastic tempestites.

Member 3 begins with a medium-bedded bioclastic limestone with mud intraclasts up to 12 cm in size, passing upward to brachiopod-rich biocalcirudites and locally ferruginous to phosphatic sandy biocalcarenites with NE/SW-oriented, straight-crested wave ripples, interbedded with marly limestones and marlstones. The richly bioclastic layers are interpreted as tempestites, including mixed autochthonous and allochthonous fossils (algae, bivalves, brachiopods, conularids, crinoids, benthic foraminifers, gastropods, scaphopods, bryozoans, ostracodes). Vertebrate remains are also common, mostly represented by durofagous fishes feeding on shallow-water molluscs. The interbedded marlstones, instead, contain chiefly infaunal bivalves and quasi-infaunal productids.

The three members of the Khuff Formation are still recognized in the Jabal Gharif area, where the sandy fraction is more abundant. The base of the Khuff Formation is here placed at the base of bioclastic hybrid sandstones with wave ripples, sharply followed by bioclastic limestones with encrusting bryozoans (Fig. 5). Member 1 is much thinner, consisting of coarse-grained sandy and bioclastic limestones interbedded with nodular limestones. Sandy biocalcarenites with wave ripples still occur locally in Member 2. Member 3 is similar throughout the Haushi–Huqf area, where its base is again marked by a conspicuous quartzose bio-intracalcarenite bed, with intraclasts up to 14 cm in size.

3.2. Sandstone petrography

Up to coarse-grained, moderately well-sorted sandstones with few bioclasts (brachiopod spines and shells, phosphate remains) occur only in Member 1 of the Khuff Formation, the sand fraction being mostly absent in Members 2 and 3. At Jabal Gharif, a medium-grained hybrid sandstone, with microsparitic pseudomatrix and subordinate silicified brachiopods and bivalves representing 29% of the rock, marks the base of Member 3.

The Khuff sandstones are all quartz-rich K-feldspar subarkoses (Q 91–95; F 5–9; L 0–2; parameters after Dickinson, 1970). Detrital quartz is mostly monocrystalline (90–96% of the grains) and commonly rounded (2–19% of the grains in sandstones and up to 33% in hybrid arenites). Feldspars mostly include twinned microcline (31–100% of total K-feldspars) and commonly perthitic orthoclase. Albitized K-feldspar to chessboard-albite, or kaolinite patches representing leached feldspar grains also occur. Plagioclase is rare to absent ($P/F \leq 7$). Sporadic rock fragments include granitoid, felsic volcanic, and metamorphic (quartz–muscovite) grains. Dense minerals include abundant and commonly rounded tourmaline, with subordinate zircon and rutile. Muscovite occurs.

Authigenic calcite is invariably abundant, accounting for 25–38% of the rock in Member 1 and reaching 49% in hybrid sandstones of the upper part of the unit. Porosity is significant ($\leq 20\%$). Quartz to feldspar overgrowths occur on some grains.

Fig. 5. Stratigraphic section of the Khuff Formation in the Jabal Gharif area, starting at 19°57′01″N 57°21′38″E. Only the uppermost brachiopod assemblage biozone has been identified, the brachiopods being much less diversified than those in the Haushi–Saiwan area. Legend as in Fig. 3.

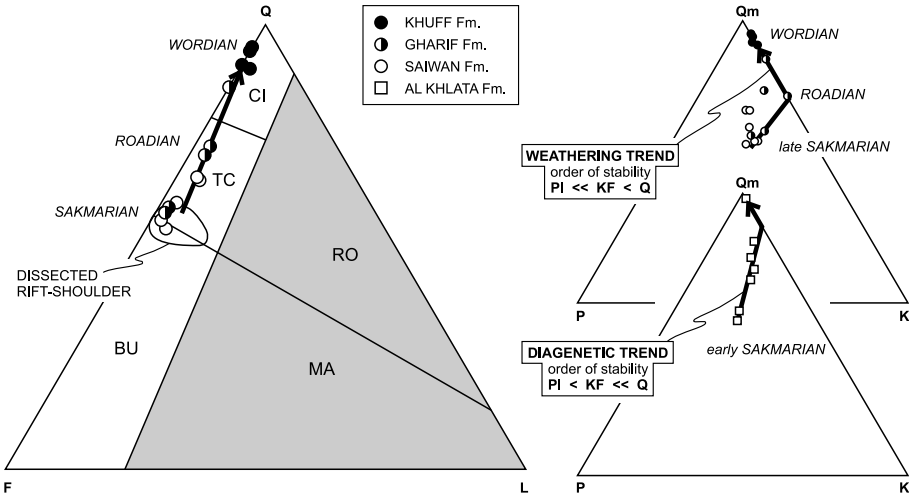

Fig. 6. Composition of Permian sandstones was strongly affected by both pre- and post-depositional selective destruction of unstable grains. The distinct trend from two-feldspar arkose in the Lower Permian to quartz-rich K-feldspar subarkose in the Middle Permian suggests increasing chemical weathering of plagioclase, ascribed in turn to both warming climates and reduced relief after opening of Neotethys. Variations in mineralogic stability within single stratigraphic units (e.g. Al Khlata Formation), instead, mostly reflect diagenetic leaching; in this case plagioclase appears to dissolve only slightly faster than K-feldspar. Plots and provenance fields after Dickinson (1985): BU = basement uplift; TC = transitional continental; CI = craton interior; RO = recycled orogen; MA = magmatic arc. Field for 'dissected rift-shoulder provenance' after Garzanti et al. (2001).

3.2.1. Provenance

The Khuff sandstones plot in the 'continental block, craton interior provenance' (Dickinson, 1985; Fig. 6), which would be consistent with a scenario of relative tectonic quiescence, progressively reduced topographic relief, and peneplanation of rift highlands in an advanced post-rift stage, when wider drainage basins allowed longer-distance sediment transport across continental lowlands.

Extrabasinal detritus largely consists of angular to subrounded quartz grains. A distinct population of rounded quartz (locally displaying reworked overgrowths) and ultrastable dense minerals occurs, but the Q_r/Q ratio is not higher than that observed in modern Yemen sands derived from the dissected shoulder of the Gulf of Aden rifted margin, where basement rocks are extensively exposed (Garzanti et al., 2001). It can be assessed that conservatively about 15% of total detritus was provided by recycling of older quartzose sediments, possibly exposed along the Haushi–Huqf arch.

Occurrence of feldspars and rock fragments from igneous to high-grade metamorphic sources indicate provenance from Pan-African basement rocks, but unstable grains were selectively altered and destroyed due to the combined effects of chemical weathering, mechanical breakage during transport, and diagenesis (Fig. 7a; McBride, 1985; Dutta, 1992; Johnsson, 1993). Alteration of detrital feldspars in soils is indicated by dissolution pits and re-entrants (Cleary and Conolly, 1972; Suttner and Dutta, 1986), including kaolinite-filled embayments (Fig. 7b,c). Solution and replacement in diagenetic environments is documented by feldspar grains with saw-tooth terminations, testifying to preferential leaching along cleavage planes (Fig. 7d), by development of secondary porosity, or by authigenic calcite locally engulfing framework grains.

3.3. Depositional environment

Member 1 of the Khuff Formation represents the onset of carbonate shelf sedimentation along the Haushi–Huqf, documenting a major regional transgressive event. The organic-rich, marsh–alluvial to estuarine environments of the uppermost Gharif Formation were replaced by paralic to

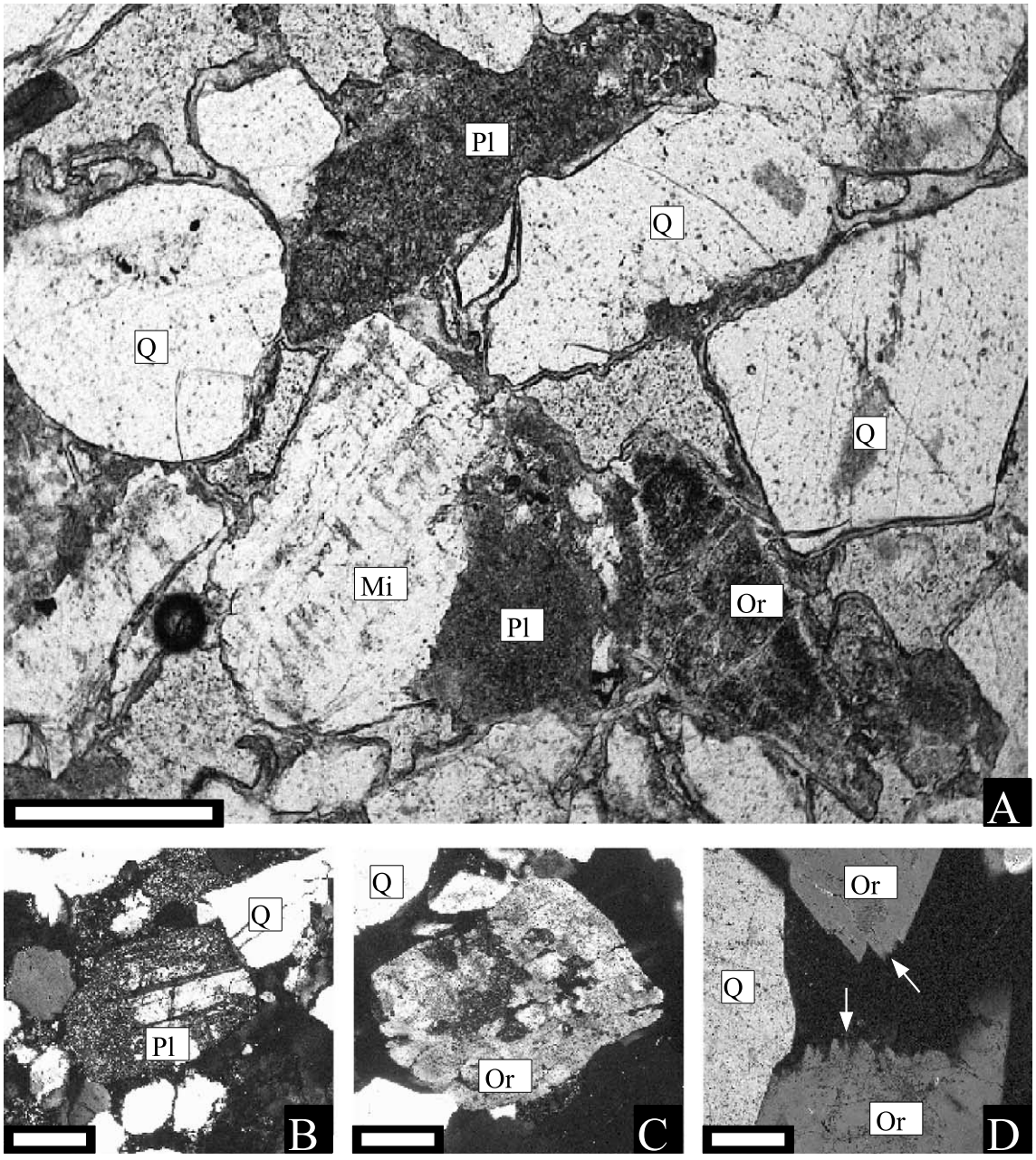

Fig. 7. Different stability of quartz and feldspar grains in the Middle Permian Gharif Formation. (A) Alteration is complete for plagioclase (Pl), advanced for orthoclase (Or), incipient for microcline (Mi), and negligible for quartz (Q), documenting the order of stability Pl < Or < Mi < Q. (B) Advanced pre-depositional? argillification of twinned plagioclase. (C) Pre-depositional? solution pits in detrital orthoclase. (D) Saw-tooth terminations of orthoclase grains (arrows), indicating extensive post-depositional dissolution along cleavage planes. Photos B–D with crossed polars. Scale bar = 250 μm.

coastal sands interpreted as tidal sand-flat to barrier-beach deposits (unit C), variably reworked by waves and tidal currents in a lagoonal or bay environment (Crumeyrolle et al., 1997). Unit C records the rapid retrogradation of the fluviatile system and a major change in basin topography during the transgression. It marks the transition between the top of the Gharif Formation, when river discharge was very important, and unit D, when carbonate sedimentation became progressively dominant as the river system retreated further inland.

Unit D consists of inner- to outer-shelf sediments deposited at water depths mostly comprised between fair-weather-wave-base and exceptional-storm-wave-base.

Member 2 of the Khuff Formation, characterized by limestones and marlstones with open marine fauna, records transition to outer-shelf conditions mostly below storm-wave-base. Thin layers of distal tempestites occur, regularly spaced about every 10 calcareous beds, suggesting control by astronomic cycles.

Abundance of bioclastic storm layers in Member 3 points to deposition around storm-wave-base. Storm-generated currents frequently affected the sea-bottom at water depths of a few tens of meters. Sedimentary features in the topmost beds of the member suggest even shallower waters, above storm-wave-base. The coastline of the Interior Oman basin, as indicated by sedimentary structures, was consistently oriented NE/SW throughout deposition of the Khuff Formation, roughly parallel to the Haushi–Huqf uplift. The consistent clastic supply suggests that river discharge was significant during the deposition of the formation.

The evolution of depositional environments is supported by the taphonomic analyses of the fauna. Member 1, characterized by abundance of chonetids and chonetellins and shell beds including both fragmented and articulated specimens with convex-upward ventral valves, indicates winnowing of the fine fraction and in situ concentration of shells by storm waves. Member 2, dominated by quasi-infaunal spiny productids, suggests instead significantly deeper-water muddy bottoms, only exceptionally affected by storms. Shallower-water conditions and turbulent bottoms affected by stronger storm action, are indicated for Member 3, including mostly disarticulated attached species (e.g. richthofenioids, terebratulids, spiriferinids) with overall higher diversity. Conodonts confirm open marine conditions throughout the unit.

Tempestites in both Members 1 and 2 record mixing of shallow-water fauna (attached or coarse-substratum-adapted brachiopods, gastropods, nuculids and other bivalves, crinoids, both *Rugosa* and *Tabulata* corals, bryozoans, barnacles, ostracodes) with relatively deeper-water autochthonous forms (quasi-infaunal productids, infaunal bivalves, large bellerophontids). Shells of autochthonous elements (especially productids) are typically found convex-upward at the top of the beds, indicating shell reworking during storm events. The occurrence of very shallow-water ostracodes with closed carapaces also suggests mass transport to deeper waters during storm events. Fish remains from the Khuff Formation chiefly consist of isolated teeth, scales and dermal denticles, and bones of durophagous fishes, both condrychthyans and osteichthyans.

Although fish remains have been found throughout the formation, the richest samples come from shell-beds in which shallow-water dwellers have been concentrated. In fact, most fishes lived in shallow waters feeding on molluscs: their remains could have been locally reworked, as testified by the different preservation of specimens in the same bed, before being definitively buried during major storm events.

Very significant is the transition from distal to proximal tempestites in the poorly exposed topmost part of Member 3. These bioclastic beds are rich in mostly disarticulated molluscs and brachiopods of the *Grandaurispina ghabaensis–Kozlowskia tescorum* Biozone and in large turriculated gastropods, pointing to a rapid transition toward shallower environments.

The same transgressive–regressive trend is recognized in Jabal Gharif, where the Khuff Formation was deposited in much shallower proximal settings, as indicated by more abundant terrigenous detritus and widespread wave ripples. Brachiopod faunas dominated by pedicle-attached

forms and virtually lacking quasi-infaunal productids also testify to shallower, turbulent-water conditions. Numerous specimens of *Lingula* at the top of the formation may indicate a trend toward more unstable settings, with variation of salinity and clastic supply. A more proximal setting for the Jabal Gharif is also supported by the rapid and frequent variation in the ostracod fauna.

4. Paleontology and biostratigraphy

Very rich fossiliferous levels are widespread throughout all the members and are particularly abundant in Member 1 and in the lower part of Member 3. If some groups are noted for their abundance and preservation and have already been described by Hudson and Sudbury (1959) and Miller and Furnish (1957), others, such as algae, pseudoalgae, conularids, crinoids, bryozoans, corals, foraminifers, trilobites, and vertebrate remains, are rarer or not yet fully studied. For instance, foraminifers are represented by 11 species of Miliolina, Rotaliina and Endothyrida, whereas algae and pseudoalgae respectively consist of *Permocalculus* cf. *tenellus* and *Stacheoides* sp. (Vachard, in Angiolini et al., 1998).

The varied fauna of the Khuff Formation is of particular importance in establishing mid-Permian correlation. In fact, the concomitant occurrence of conodonts, brachiopods, ammonoids, bivalves and foraminifers make correlation easy both with the paleotropic and the high-latitude regions. The southeastern Oman fauna can thus be correlated with the mid-Permian faunas from Iran to South Thailand and with the Guadalupian of West Texas.

4.1. Ammonoids

Ammonoids occur only spodarically in the Khuff Formation of the Huashi area. The most significant findings (sample OL6) come from the topmost 2.5 m of Member 2 nearby section I4 (Fig. 3), where numerous (about 70 specimens) and well preserved specimens of *Pseudohalorites arabicus* Miller and Furnish, 1957 have been collected together with nautilocon nautiloids. The ammonoid specimens fit very well for preservation as well as morphology with the up to now unique specimen described in the species *P. arabicus* by Miller and Furnish (1957). Other species of the genus are reported from the Chihsia Formation of South China. Three specimens of *Stacheoceras* sp. have also been detected from sample OM16 along the Haushi I1 section. *Stacheoceras* is a long-ranging form with a widespread paleogeographic distribution and it occurs also in the red cephalopod limestones of Rustaq in North Oman (Blendinger et al., 1992).

From the taphonomic point of view, the cephalopods display several features related to deposition and burial under the influence of currents: size sorting (*Pseudohalorites arabicus* from 16 to 27.5 mm in diameter, with maximum frequency at 22–24 mm), differential and incomplete filling of the chambers of phragmocones, and secondary filling channel through septal necks (Hagdorn and Mundlos, 1983).

4.2. Brachiopods

The brachiopod fauna (Pl. I; Table 1a,b) of the Khuff Formation is highly diversified and numerically dominated by the quasi-infaunal productids *Celebetes manarollai* Angiolini in Angiolini and Bucher (1999), *Dyschrestia rugosa* Angiolini in Angiolini and Bucher (1999), *Juresania omanensis* Hudson and Sudbury, 1959 and *Linoproductus* aff. *kaseti* Grant, 1976. Terebratulids belonging to the genus *Dielasma* are also common. The chonetid *Neochonetes* (*Nongtaia*) *arabicus* (Hudson and Sudbury, 1959) is locally very abundant. The productids *Kozlowskia tescorum* (Hudson and Sudbury, 1959), *Bilotina yanagidai* Angiolini in Angiolini and Bucher (1999) and *Grandaurispina ghabaensis* Angiolini in Angiolini and Bucher (1999), the orthid *Orthotichia* cf. *bistriata* Reed, 1944, the strophomenids *Perigeyerella raffaelae* Angiolini in Angiolini and Bucher (1999) and *Derbyia* cf. *diversa* Reed, 1944, and the spiriferinids *Spiriferellina* and *Callispirina* are subordinated. Specimens of *Haydenella* sp., *Vediproductus* sp. [= *Calliprotonia* sp. in Angiolini and Bucher (1999)], *Magniplicatina* sp., ?*Cyclacantharia* sp., *Globosobucina* sp., *Acritosia* sp., *Edriosteges* sp.,

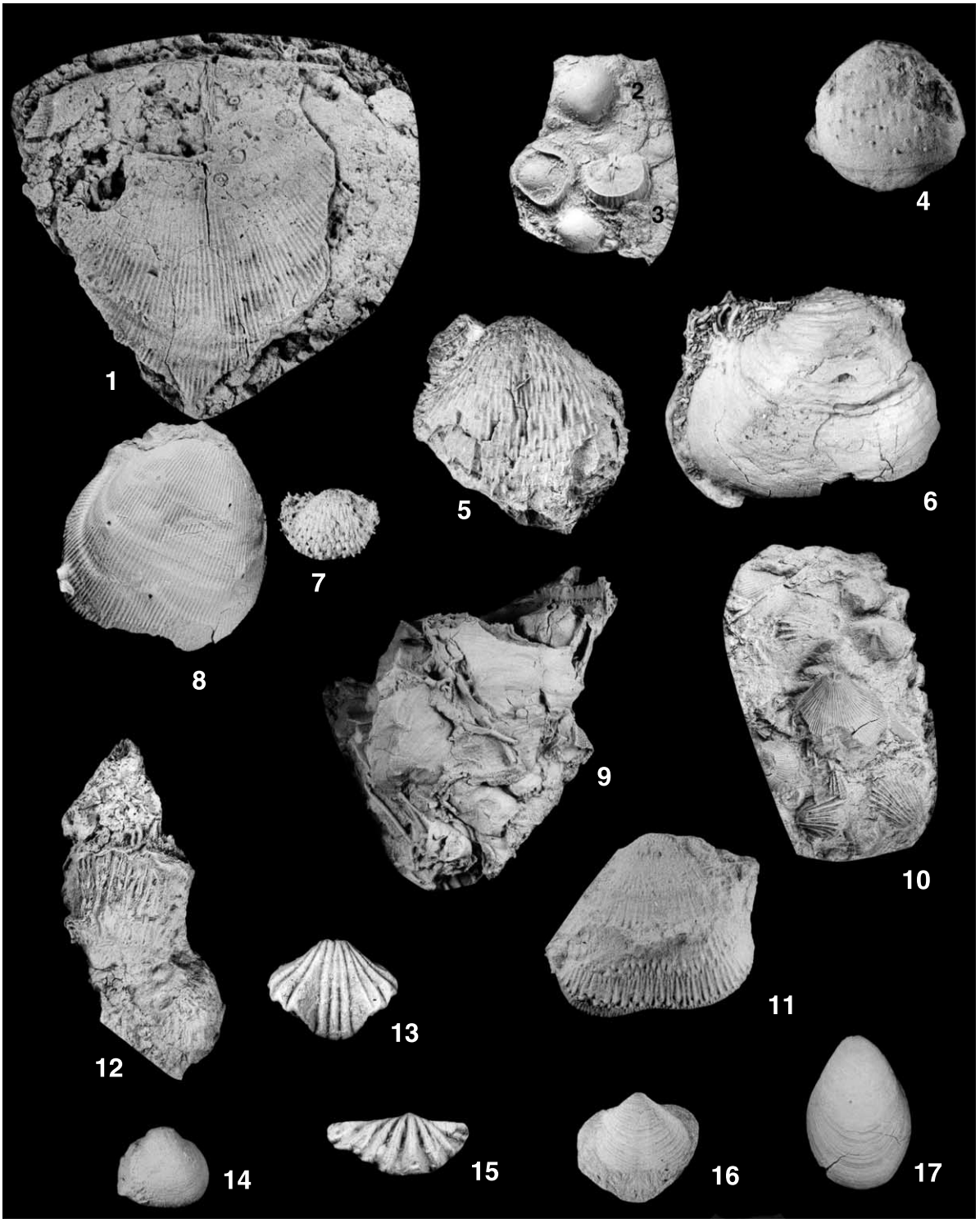
1
2
3
4
5
6
7
8
9
10
11
12
13
14
15
16
17

?*Darlinuria* sp., *Terebratuloidea* sp., *Cleiothyridina* cf. *seriata* Grant, 1976, *Squamularia* sp., *Martiniopsis* sp., and *Hemiptychina* sp. are rare. The composition of the overall fauna varies moving from the Haushi area southward to the Jabal Gharif. In the latter region, in fact, the diversity is much lower and the brachiopod fauna is dominated by pedicle-attached forms such as *Lingula* sp., *Dielasma* spp., *Orthotichia* cf. *bistriata*, *Cleiothyridina* cf. *seriata* and *Squamularia* sp. (Fig. 5; Table 1a,b).

The Khuff brachiopod fauna is a transitional fauna sensu Shi et al. (1995), comprising wide-ranging (*Orthotichia*, *Derbyia*, *Linoproductus*, *Cleiothyridina*, *Martiniopsis*, *Spiriferellina*, *Dielasma*), paleoequatorial (*Perigeyerella*, *Haydenella*, *Kozlowskia*, *Edriosteges*, *Grandaurispina*, *Acritosia*, *Terebratuloidea*, *Squamularia*, *Hemiptychina*), Gondwanan (*Dyschrestia*, *Callispirina*) and endemic genera (*Celebetes*, *Bilotina*, *Vediproductus*, *Globosobucina*). This assemblage shows strong affinities with the brachiopods of the Amb Formation of the Salt Range in Pakistan (Waagen, 1882–1885) and those of the Rat Buri Limestone of South Thailand (Grant, 1976).

The biochronologic analysis of the Khuff brachiopods in the Haushi sections led to the establishment of a local biochronologic sequence of eight faunal associations (Angiolini and Bucher, 1999), based on the Unitary Associations method of Guex (1991). This analysis pointed out that if facies had a clear influence on the quantitative distributions of the brachiopod assemblages as well as on species diversity, some taxa were not strictly facies-controlled, their occurrence being independent on the sedimentary evolution. It is noteworthy that *Dyschrestia rugosa* and *Bilotina yanagidai* are not strictly facies-controlled, their FADs being linked to the deepening of the environment but their range extending up into regressive shallow-water deposits. The same holds true for *Celebetes manarollai*, which only occurs in the most contrasted facies of the first and second members. *Orthotichia* cf. *bistriata* and *Neochonetes* (*Nongtaia*) *arabicus* are restricted to the shoreface deposits of Member 1, but do not reappear in Member 3: their last appearance may thus be a potential biochronologic marker. The first occurrences of the genera *Edriosteges*, *Globosobucina*, *Terebratuloidea*, *Martiniopsis* and *Squamularia* in Member 3 may also represent potential biochronologic markers. *Perigeyerella raffaellae*, *Derbyia* cf. *diversa*, *Linoproductus* aff. *kaseti* and *Juresania omanensis* are the only species that range throughout the eight Unitary Associations. *P. raffaellae* and *Derbyia* cf. *diversa* are both

Plate I. All figured specimens are housed at Dipartimento di Scienze della Terra, Università degli Studi di Milano, Milan, Italy. All natural size.

1 *Derbyia* cf. *diversa* Reed, 1944, ventral valve; sample OL13.
2 *Celebetes manarollai* Angiolini in Angiolini and Bucher, 1999, ventral valve; sample AO80.
3 *Bilotina yanagidai* Angiolini in Angiolini and Bucher, 1999, dorsal valve interior; sample AO80.
4 *Dyschrestia rugosa* Angiolini in Angiolini and Bucher, 1999, ventral valve; sample OL38.
5 *Juresania omanensis* Hudson and Sudbury, 1959, ventral valve; sample AO210.
6 *Edriosteges* sp., ventral valve; sample AO210.
7 *Grandaurispina ghabaensis* Angiolini in Angiolini and Bucher, 1999, ventral view of an articulate specimen, sample OL51.
8 *Linoproductus* aff. *kaseti* Grant, 1976, ventral valve; sample OM16.
9 *Globosobucina* sp., three cemented ventral valves; sample AO210.
10 *Perigeyerella raffaellae* Angiolini in Angiolini and Bucher, 1999 two ventral valves with bivalves; sample AO210.
11 *Vediproductus* sp., ventral valve; sample 526E.
12 *Acritosia* sp., two ventral valves; sample AO210.
13 *Terebratuloidea* sp., ventral valve; sample AO210.
14 *Orthotichia* cf. *bistriata* Reed, 1944, ventral view of an articulate specimen; sample AO111.
15 *Spiriferellina* sp., dorsal view of an articulate specimen; sample AO210.
16 *Cleiothyridina* cf. *seriata* Grant, 1976, ventral view of an articulate specimen; sample JPP392A.
17 *Dielasma* sp., ventral view of an articulate specimen; sample AO113.

Table 1a
Range charts of brachiopods and conodonts. Haushi K7 section

	Brachiopods																					Conodonts				
Sample	*N. (N.) arabicus*	*C. manarollai*	*L. aff. kaseti.*	*D. rugosa*	*B. yanagidai*	*O. cf. bistriata*	*J. omanensis*	*Vediproductus* sp.	*Acritosia* sp.	*Edriosteges* sp.	*Globosobucina* sp.	*Terebratuloidea* sp.	*Spiriferellina* sp.	*Dielasma* spp.	*P. raffaellae*	*D. cf. diversa*	*Haydenella* sp.	*G. ghabaensis*	*Martiniopsis* sp.	*?Squamularia* sp.	*Callispirina* sp.	*K. tescorum*	*Merillina* sp.	*Hindeodus* sp.	*H. wordensis*	*ramiforms*
AO72			x				x								x	x						x				x
AO73			x				x				x	x	x	x		x	x	x	x	x	x	x			x	
OM44																								x		
AO76							x								x	x										
AO210							x		x	x	x	x	x	x	x											
OM43																										x
OM41																										x
OM40																										x
AO82								x	x													x		x	
OL201		x						x																		
AO80	x	x		x	x	x	x																			
OL202	x	x	x																							
OL200	x																									
Haushi K7																										

absent from the offshore second member, but *J. omanensis* and *L.* aff. *kaseti* are recorded from all three members.

The eight faunal associations of Angiolini and Bucher (1999) are here grouped into three assemblage zones: the *Neochonetes* (*Nongtaia*) *arabicus*–*Celebetes manarollai* Biozone (grouping Unitary Associations 1–5), the *Acritosia* sp.–*Globosobucina* sp. Biozone (Unitary Association 6) and the *Grandaurispina ghabaensis*–*Kozlowskia tescorum* Biozone (Unitary Associations 7 and 8) (Figs. 2–5). The first assemblage zone characterizes chiefly Member 1, rarely ranging up to Member 2; the *Acritosia* sp.–*Globosobucina* sp. Biozone ranges from Member 2 to Member 3, whereas the third biozone characterizes the topmost outcropping part of Member 3. All the biozones are separated by barren intervals (Fig. 2).

4.3. Conodonts

Following the paper by Angiolini et al. (1998), new sections have been sampled and studied for conodont researches, but the conodont fauna from the Khuff Formation is not particularly abundant, with elements often broken. Sample size ranged from 3 to 5 kg. The conodont elements extracted are mostly ramiforms, Pa elements are less abundant and belong to the genera *Hindeodus* and *Merrillina*. The color of conodonts from all the sections is straw or pale orange, approximating to a color alteration index (CAI) of 1.0–1.5 (Epstein et al., 1977; Rejebian et al., 1987) that indicates very little post-burial heating (less than 50–80°C).

The following events have been detected in the conodont fauna that are very monotonous all along the Khuff Formation (Pl. II; Table 1a,b):

– The lower/middle portion of the formation (Members 1 and 2) yielded ramiform and Pa elements belonging to *Hindeodus wordensis* Wardlaw, 2000, *Merrillina praedivergens* Kozur and Mostler, 1976 and *Sweetina* sp. In Angiolini et al. (1998) only 2 Pa elements of *Merrillina* were found at the base of Member 2 (OL27) and were attributed to *Merrillina praedivergens* Kozur and Mostler mainly on the basis of a 'thick, long cusp posteriorly directed and weakly inclined toward the base, with three massive, thick, short denticles, partly fused in two in the middle'. After the new researches, few other Pa elements of *Merrillina* have been found. These elements, with re-

Table 1b
Range charts of brachiopods and conodonts. Haushi I1, Saiwan and Jabal Gharif sections

	Brachiopods								Conodonts			
Sample	*P. raffaellae*	*D. cf. diversa*	*N. (N.) arabicus*	*J. Omanensis*	*L. aff. kaseti.*	*O. cf. bistriata*	*Dielasma* spp.	*C. manarollai*	*Acritosia* sp.	*D. rugosa*	*Merillina* sp.	*H. wordensis*
OM12bis		x										
OM12	x											
OM14					x					x		
OM13										x		
OM16					x			x	x	x		
OM11		x				x	x	x				
OM10											x	x
OM10bis	x	x	x	x	x	x		x				
0M15		x			x	x	x					
Haushi I1												

	Brachiopods							Conodonts		
Sample	*P. raffaellae*	*N. (N.) arabicus*	*L. aff. kaseti.*	*D. cf. diversa*	*J. omanensis*	*K. tescorum*	*C. manarollai*	*Dielasma* spp.	*M. praedivergens*	*Hindeodus* sp.
AO130		x			x		x	x		
AO129									x	x
AO128		x			x		x			
A0131			x							
AO127						x				
AO125				x		x				
AO126				x	x					
AO124	x	x	x							
Saiwan										

	Brachiopods					Conodonts				
Sample	*Dielasma* spp.	*Juresania* sp.	*O. cf. bistriata*	*C. cf. seriata*	*Squamularia* sp.	*Lingula* sp.	*M. praedivergens*	*Hindeodus* sp.	*H. wordensis*	*ramiforms*
AO202						x				
AO204						x				
AO206						x				
AO116										x
AO115									x	x
AO114									x	
AO113	x			x	x			x		x
AO112	x			x	x					
AO111	x	x	x	x						
AO109	x									
OL105	x									
AO102							x			
Jabal Gharif										

spect to the previous ones, show more discrete denticles, but massive and a thick, not particularly high cusp clearly posteriorly inclined. These elements may represent transitions or intraspecific variations to *Merrillina divergens* (Bender and Stoppel, 1965) (Pl. II). On the consideration previously esposed, we distingush two different species [*Merrillina praedivergens* Kozur and Mostler and *Merrillina divergens* (Bender and Stoppel)]. According to Swift and Aldrige (1982) and Wardlaw and Collinson (1986) *Merrillina praedivergens* is = to *M. divergens* (Bender and Stoppel). The Pa elements of *Hindeodus excavatus* Behnken sensu Wardlaw and Collinson (1984) mentioned and illustrated in Angiolini et al. (1998) are here attributed to *Hindeodus wordensis* Wardlaw after the paper by Wardlaw (2000) came out because of the 'large cusp much higher than denticles; denticles increasing in width posteriorly, except for posteriormost, and generally decreasing in height posteriorly, except for posteriormost three which may be of subequal height' (Pl. II).

– In Member 3, ramiform elements belonging to *Merrillina* sp., *Hindeodus* sp., *Sweetina* sp. and 1 Pa elements of *Hindeodus wordensis* Wardlaw have been found.

The conodont association from the Khuff Formation indicates shallow-water conditions.

4.4. Ostracodes

Thirty five species belonging to 18 genera were identified and figured in Crasquin-Soleau et al. (1999). Ten new samples collected in the Jabal Gharif section contain ostracodes extracted from the sediments by hot acetolysis (Lethiers and Crasquin-Soleau, 1988). This ostracod fauna is composed of about 700 specimens belonging to 17 species and 10 genera (Pl. III; Table 2). Almost all the species found here were also present in the northern cliff of the Haushi area (Crasquin-Soleau et al., 1999). According to Melnyk and Maddocks (1988), Peterson and Kaesler (1980), and Costenzo and Kaesler (1987), the ostracod genera encountered are known to be benthic, shallow-marine forms. More specifically, the Bairdiacea are present in shallow to deep, open carbonate environments with normal salinity. The Cavellinidae

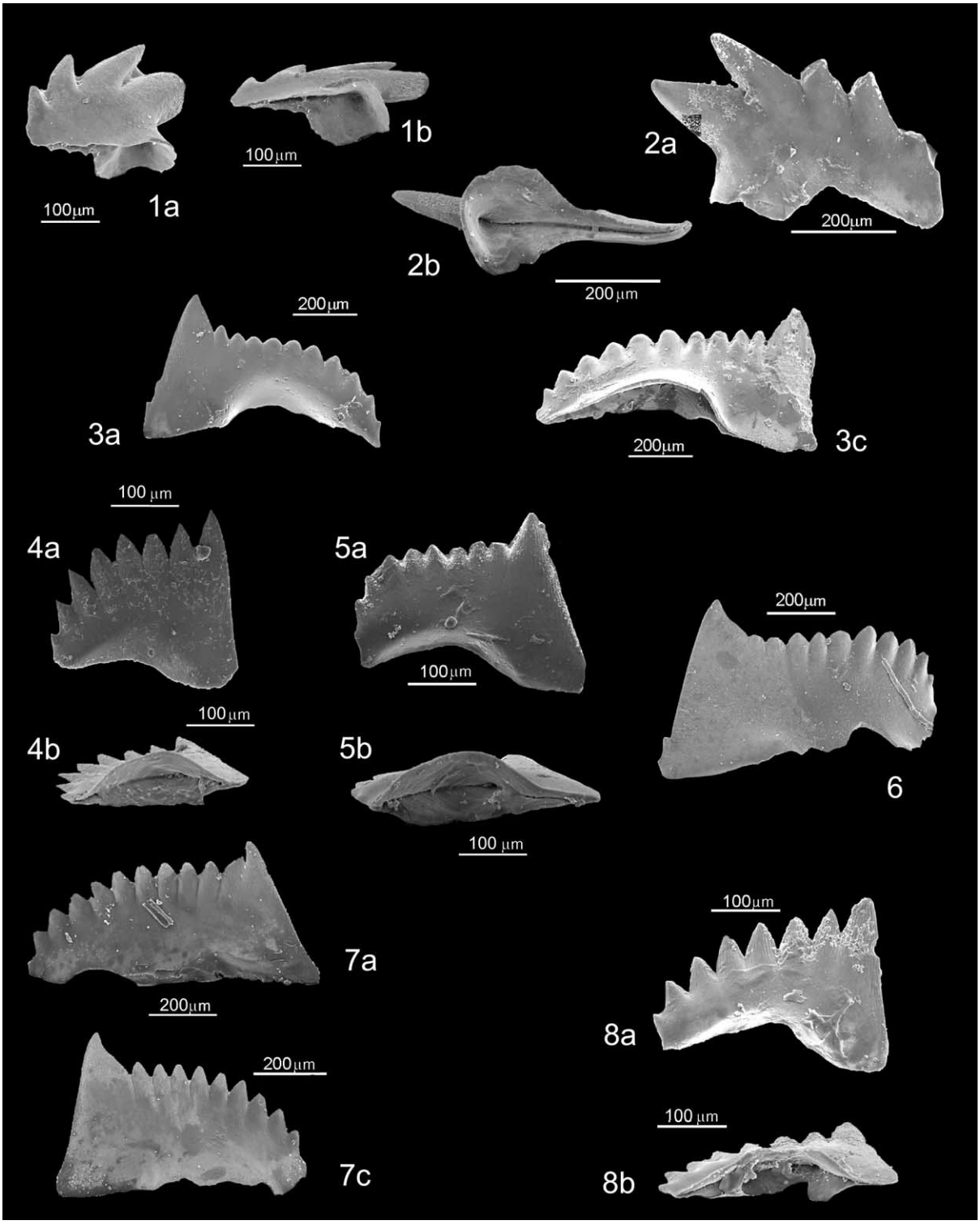
1a
100μm
1b
100μm
2a
200μm
2b
200μm
3a
200μm
3c
200μm
4a
100 μm
4b
100μm
5a
100μm
5b
100 μm
6
200μm
7a
200μm
7c
200μm
8a
100μm
8b
100 μm

Table 2
Range charts of ostracodes species along the Jabal Gharif section

Sample	Number of specimens	*Cavellina huqfensis*	*Hollinella (H.) herrickana*	*Hollinella (H.) martensi*	*Bairdia* sp. 2	*Knightina umoda*	*Knoxites* cf. *brevirostris*	*Roundyella suboblonga*	*Sargentina minuta*	*Sulcella sulcata*	*Bairdia* sp. 1	*Sulcella arabica*	*Sargentina woutersi*	*Cavellina boomeri*	*Cavellina gerryi*	*Fabalicypris parva*	*Geffenina wangi* n.sp.	*Hollinella benzartiae*	*Fishes*
00AO102	275		XXX	XXXX										X			X	X	
00AO103	5		X	X										–			–		
00AO104	43		X	X										XXX	X	X	–		
00AO105	11		XX	–										–	–	–	–		
00AO106	55		XXX	–									X	–	–	–	X		
00AO107	116		X	X					X	X	X	X	–	–	X	X	XXXX		
00AO110	2		X	–					–	–	–	–	–	–					
00AO113	43	X	XX	XX	X	X	X	X	XX	X	X	X	XX	X					
00AO115	140	–	XXXX	XX															
00AO116	8	X	XX																

XXXX: very abundant (>70 specimens).
XXX: abundant (30–70 specimens).
XX: present (5–30 specimens).
X: rare (1–5 specimens).
–: presence supposed.

were adapted to very shallow to shallow euryhaline environments. The Kloedenellacea dwelled in very shallow, euryhaline environments. The Kirkbyidae spread out in subtidal, normal-marine environments. The large species of Hollinacea with developed adventral structures characterize environments such as interdistributary bay, prodelta and interdeltaic embayments, and lagoons. The repartition of the species in percentage of families and/or superfamilies in the Jabal Gharif section is the following:

– the Bardiacea are very rare (present only in three samples with a maximum of 4.7% of specimens in sample AO113);

– the sublittoral Kirkbyidae occur in sample AO113 and represent 7% of specimens;

– the Cavellinidae occur in quite all the samples with percentages varying from 0.4% to 88.6% of specimens; the Kloedenellacea are represented in 4 samples and reach 87.9% in sample AO107; the Hollinacea are present in all the samples and vary from 3.4% to 100% of specimens. These three family and superfamilies dominate greatly the ostracod gathering.

Plate II. All figured specimens are housed at Dipartimento di Scienze della Terra, Università degli Studi di Milano, Milan, Italy. Magnifications indicated by bar.

1a,b *Merrillina praedivergens* (Kozur and Mostler), transition to *Merrilina divergens* (Bender and Stoppel), sample AO102; Pa element: (a) lateral view, (b) oblique/lower view.
2a,b *Merrillina praedivergens* (Kozur and Mostler), sample AO129; Pa element: (a) lateral view, (b) lower view.
3a,c *Hindeodus wordensis* Wardlaw, sample AO79; Pa element: (a,c) lateral views.
4a,b *Hindeodus wordensis* Wardlaw, sample AO79; Pa element, early growth stage: (a) lateral view, (b) lower view.
5a,b *Hindeodus wordensis* Wardlaw, sample AO79; Pa element, early growth stage: (a) lateral view, (b) lower view.
6 *Hindeodus wordensis* Wardlaw, sample AO82; Pa element, lateral view.
7a,c *Hindeodus wordensis* Wardlaw, sample OM21; Pa element: (a,c) lateral views.
8a,b *Hindeodus wordensis* Wardlaw, sample AO73; Pa element: (a) lateral view, (b) lower view.

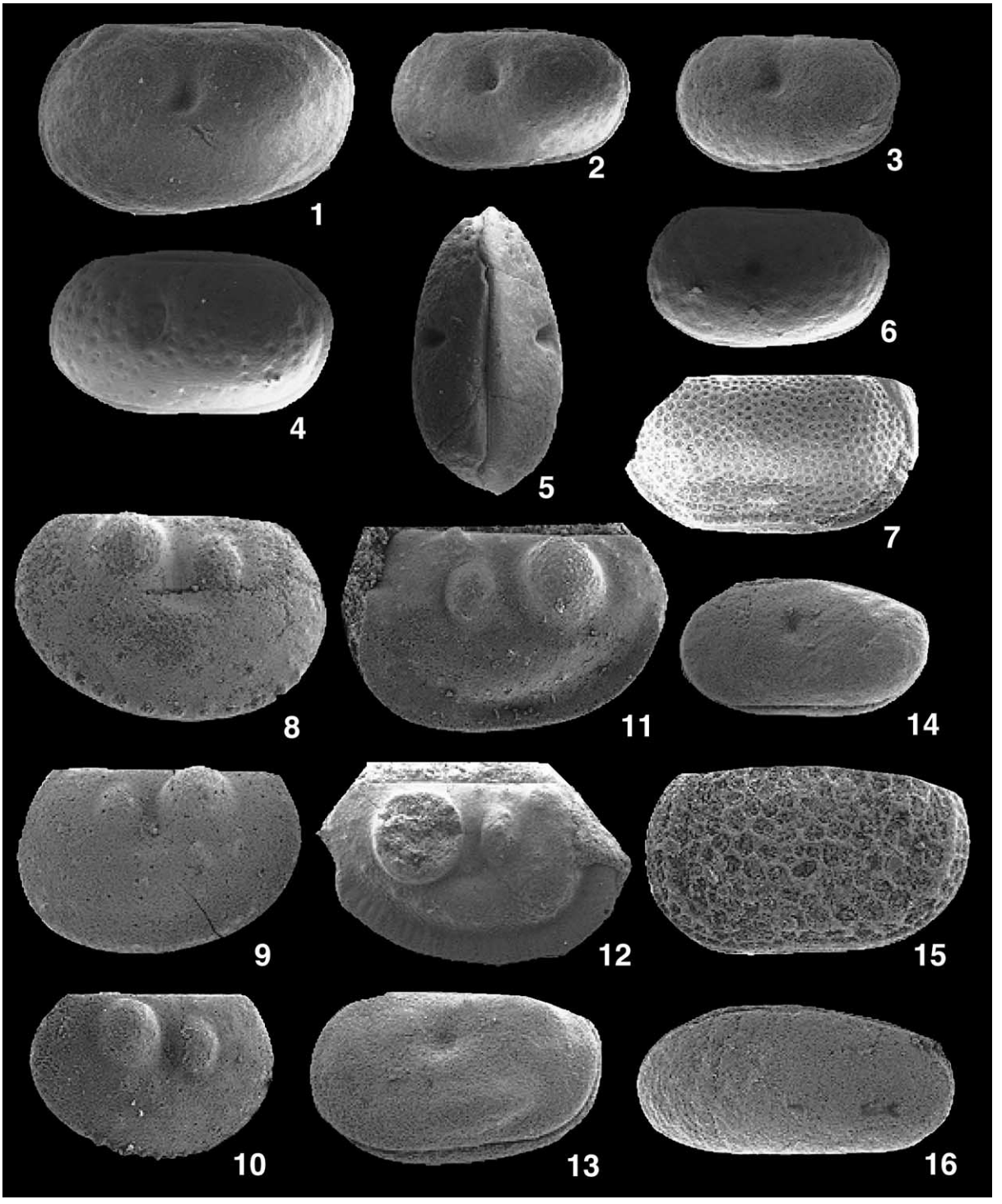
1
2
3
4
5
6
7
8
11
14
9
12
15
10
13
16

Almost all of the specimens are closed carapaces, and they generally occur only as adults and the last larval stage. It is also important to note the relatively low diversity of the assemblage and that some species are represented by a very high number of specimens, like *Hollinella* (*H.*) *herrickana* (Pl. III, 11, 12) and *Hollinella* (*H.*) *martensi* (Pl. III, 8–10), suggesting brackish, marginal-marine environments. The variations in the ostracod assemblage along the Jabal Gharif section are rapid and frequent. This could be explained by the proximal position of the original site of the ostracodes. In such a shallow, high-energy location, the modifications of life conditions (salinity, oxygenation, amount of sediment in suspension, temperature, etc.) could be frequent and reversible.

4.5. Vertebrates

Vertebrate remains such as bones, teeth, scales and dermal denticles of different kinds of fish have mostly been detected in the tempestites (Table 3), which probably concentrated the organic remains. Wear and color of the vertebrate remains can be rather different even inside the same bed, suggesting a rather long reworking period before the storm struck the shallow waters, causing the remains to resettle on deeper bottoms. However, also most of the conodont samples taken in the calcareous marls yield such vertebrate remains, though the composition of the single assemblages may vary.

Teeth of *Polyacrodus* and *Lissodus*-type are very common at the very base of Member 3, but rare in most of the others. Most teeth are massive and about 2 mm long. *Polyacrodus*-type teeth show a rather high, stout central cusp with one or two pairs of lateral cusplets. Usually, few strong ridges start from the cusps and the cutting edge. *Lissodus*-type teeth have a rather high central cusp. The enameloid is smooth, but in some specimens accessory cusplets are present both on the cutting edge and the labial face. The crown is well separated from the root all around through a narrow 'neck'.

Cladodont teeth are found in almost all fossiliferous samples – chiefly in the middle–upper part of Member 3 – and are locally very common. The main central cusp is flanked by two lateral cusps on each side: all the elements are commonly somewhat worn. Relative size of the cusps may vary, but usually the central is at least twice the lateral ones. Teeth with a single cusp are also present. Cusp ornamentation varies from smooth to stout ridges.

The most common remains (but very rare at the

Plate III. All figured specimens are housed at Laboratoire de Micropaléontologie, Université Pierre et Marie Curie, Paris, France.

1 *Geffenina* sp., left lateral view; P6M1435; ×80.
2 *Geffenina* sp., left lateral view; P6M1436; ×55.
3 *Geffenina* sp., left lateral view; P6M1437; ×55.
4 *Geffenina* sp., left lateral view; P6M1438; ×55.
5 *Geffenina* sp., dorsal view; P6M1439; ×55.
6 *Geffenina* sp., left lateral view; P6M1440; ×55.
7 *Knightina unnoda* (Wang, 1978), right lateral view, P6M1441; ×55; sample 00AO113.
8 *Hollinella* (*H.*) *martensi* Crasquin-Soleau in Crasquin-Soleau et al., 1999, right lateral view; P6M1442; ×80; sample 00AO102.
9 *Hollinella* (*H.*) *martensi* Crasquin-Soleau in Crasquin-Soleau et al., 1999, left lateral view; P6M1443; ×55; sample 00AO102.
10 *Hollinella* (*H.*) *martensi* Crasquin-Soleau in Crasquin-Soleau et al., 1999, right lateral view; P6M1444; ×55; sample 00AO102.
11 *Hollinella* (*H.*) *herrickana* (Girty, 1909), left lateral view; P6M1445; ×50; sample 00AO102.
12 *Hollinella* (*H.*) *herrickana* (Girty, 1909), right lateral view; P6M1446; ×45; sample 00AO1115.
13 *Perprimitia* cf *brevirostris*, left lateral view; P6M1447; ×80; sample 00AO113.
14 *Sulcella sulcata* Coryell and Sample, 1932, left lateral view; P6M1448; ×80; sample 00AO113.
15 *Roundyella suboblonga* Wang, 1978, left lateral view; P6M1449; ×110; sample 00AO113.
16 *Fabalicypris parva* Wang, 1978, left lateral view; P6M1450; ×80; sample 00AO107.

Table 3
Range charts of vertebrates along the Haushi K7, Saiwan and Jabal Gharif sections

	Menaspoid scales	Cladodont teeth	Hybodont teeth	Hybodont dentic	*Deltodus* teeth	Actinopterygian teeth	Actinopterygian scales	Actinopterygian vertebrae	"Bones"
AO72	x	x	x			x		x	x
AO73	x						x		
AO76	x								
AO210	x	x	x			x	x	x	x
Member 2		x	xx			x	x	x	x
AO82	x	x				x			
AO79			x						
Haushi K7									
OM123	x		x			x		x	x
Saiwan									
OM202	x	x	x	x		x	x		
OM204						x	x		x
OM205			x	x	x	x		xx	x
OM206			x	xx		x			x
Jabal Gharif									

base) are large menaspoid scales, the largest reaching 5 mm in length. They show a flat, commonly elongated base whith usually regular outline, although sometimes there is a single notch. No radial grooves are visible, as is the case for *Deltoptychius*, *Helodus* and *Menaspis* scales. The shape of the crown is highly variable, from thin elongated to almost round or star-shaped; only some scales are symmetric. Elongated scales, in lateral view, show a convex edge, while the other edge is straight or concave. The crown is usually made of several fused cusps, each one showing the pulp cavity when worn.

Much rarer are *Deltodus* teeth, mostly fragmentary: they have been found in two of the large samples yielding mainly menaspoid scales and cladodont teeth, as well as in a few conodont samples. These teeth are rather small (up to 7–8 mm), whereas larger fragments have been found in the arenaceous lowermost part of the Khuff Formation. Dermal denticles are also very common throughout the unit, as well as actinopterygian teeth, scales, vertebrae, and coelacanth remains.

The new fish fauna from the Khuff Formation is not only quite rich and well-preserved, but also spans a time, the Wordian, not well represented so far.

4.6. Age of the Khuff Formation

The reference scale used for the Permian System is the three-fold subdivision approved by the Permian Subcommission of ICS (Jin et al., 1997), where Guadalupian is the Middle Permian Series.

The Khuff Formation, previously considered as Late Artinskian (or not younger than Early Permian; Hudson and Sudbury, 1959), was ascribed to the middle Guadalupian, and more precisely to the Wordian [roughly corresponding to Murgabian sensu Kotlyar and Pronina (1995) (*Neoschwagerina craticulifera* Zone) of the Tethyan scale] by Angiolini et al. (1998) and Angiolini and Bucher (1999), chiefly on the basis of brachiopods and conodonts. The associated bivalves suggest the same age (Dickins, 1999).

More specifically, the *Neochonetes* (*Nongtaia*) *arabicus–Celebetes manarollai* Biozone can be assigned a Wordian age because of the occurrence of Roadian–Wordian brachiopods (*Orthotichia* cf. *bistriata*, *Derbyia* cf. *diversa*, *Linoproductus* aff. *kaseti* and the genera *Bilotina*, *Vediproductus*, *Hemiptychina*, *Celebetes*, *Perigeyerella*, *Haydenella*) together with the Wordian–Capitanian conodonts *Hindeodus wordensis* and *Merrillina praedivergens*. The conodont assemblage of the Khuff Formation is similar to those described by Wardlaw and Collinson (1984, 1986) and Wardlaw (2000) from the Word and Capitan Formations of North America, and by Wardlaw and Pogue (1995) from the Amb Formation of the Salt Range (Pakistan). The brachiopod assemblages start to differentiate in Member 3, with the overlying *Acritosia* sp.–*Globosobucina* sp. Biozone and the *Grandaurispina ghabaensis–Kozlowskia tesco-*

rum Biozone. However, the first occurrence of brachiopod genera *Edriosteges*, *Globosobucina*, *Terebratuloidea*, *Squamularia* and *Hemiptychina* still suggests a Wordian age, and the conodont assemblage is the same as occurring at the base of the formation (Table 1a,b).

The chronostratigraphic interpretation of the Khuff ammonoids is more problematic, as *Stacheoceras* is a long-ranging genus and *Pseudohalorites arabicus* is an endemic species of Interior Oman.

The uniformity in conodont and vertebrate assemblages throughout the sections (Figs. 2–5; Tables 1a,b and 3), with the absence of significant faunal turnovers, suggests that the whole Khuff Formation of Interior Oman was deposited in a short time span.

5. Climatic and paleogeographic evolution

The Lower to Middle Permian succession of the Haushi–Huqf records a significant change from glacial–arid to warm–humid climatic conditions in about 25 Myr. The Al Khlata diamictites were deposited during the earliest Permian climax of the Gondwanan glaciation, whereas the topmost interval of the unit is related to glacial retreat and concomitant sea-level rise in the late Sakmarian, with rapid evolution from glacial to temperate climates around the Tastubian–Sterlitamakian boundary (Angiolini et al., in press). The paleoflora contained in the Upper Gharif Formation suggests much warmer and humid settings at the beginning of the Middle Permian (Broutin et al., 1995), with permanent precipitation and short dry season (Fluteau et al., 2001). Such a climatic trend towards higher temperatures, inferred also for eastern Peri-Gondwanan regions (Shi and Archbold, 1995, 1998) and Western Australia (Archbold and Shi, 1995), continued during deposition of the Khuff Formation, unconformably capped by Triassic laterite/bauxite paleosols.

5.1. Paleontologic evidence for climatic change

A sharp shift in diversity and composition from the Saiwan assemblages, characterized by a clear Gondwanan signature, to the transitional Gharif and Khuff biota, is observed, reflecting a sharp change in climate from glacial–cool in the Sakmarian to warm and humid in the Wordian.

Particularly evident is the evolution in diversity and composition of brachiopod faunas below and above the warm–humid Gharif paleoflora. In fact, if on the one hand the Gharif plants clearly indicate a warm on-land climate (Broutin et al., 1995), on the other the transition from the Saiwan marine assemblages to the Khuff ones confirms a trend towards warm sea temperatures.

The Early Permian Saiwan brachiopod fauna is dominated by large and thick-shelled spiriferids with Gondwanan affinity, and has a generally low to moderate diversity, with a Permian Ratio (PR) of 0.57 (Angiolini et al., 1997). The PR is a diversity index introduced by Stehli (1970), and calculated here as amended by Shi and Archbold (1995), based on the ratio: (brachiopod families present − brachiopod cosmopolitan families found)/(brachiopod cosmopolitan families expected). Ecosystem development in the Saiwan Formation records a rapid increase in temperature at the end of the Gondwanan deglaciation, with a shift towards temperate conditions in the late Sakmarian (Angiolini et al., in press). The Middle Permian Khuff brachiopods (predominantly thin-shelled productids) are much more diversified (PR = 1.57), with a mixture of wide-ranging, paleoequatorial, Cimmerian, and Gondwanan genera indicating a consistent increase of water temperatures. Of great significance is the invasion of a large number of paleoequatorial genera (about 35%), which are good indicators of warm-water temperatures, as observed by Archbold and Shi (1995) for Permian brachiopod faunas of Western Australia. For instance, the paleotemperature curve for Western Australia, based on the diversity and composition of brachiopod genera, is consistent with the available oxygen isotopic data, and shows an increase of 10–19°C from the Asselian to the late Artinskian, and to even warmer-water temperatures at the beginning of the Middle Permian.

The occurrence of both cool-water (*Merrillina*) and warm-water (*Sweetina*) conodonts (Kozur, 1995; Wardlaw, 1995) in the Khuff Formation is

consistent with progressive warming in the Middle Permian. Furthermore, Khuff bivalves comprise genera generally associated with a silty–marly environment; they have a cosmopolitan character, and suggest mild and equable water temperatures (Dickins, 1999). Finally, Khuff ostracodes belong to the thermosphere and are typical of the intertropic zone.

All these climatic indicators suggest warm temperatures, in apparent contrast with the low diversity of foraminiferal and algal assemblages, and with the absence of calcareous sponges. Algae and foraminifers are abundant and diversified in the coeval Saiq Formation of the Oman Mountains, which is generally interpreted as a warm-water carbonate ramp/platform. However, reefs or biostroma are not recorded also in the Saiq Formation, where the level-bottom coral community has low diversity, and synsedimentary cements and biogenic incrustation are absent (Weidlich, 1999).

The low diversity of foraminifers, algae, and corals coupled with the absence of calcareous sponge may be explained by the occurrence of restrictive environmental factors such as salinity, temperature, and clastic content. The occurrence of corals, abundant molluscs, and diversified articulate brachiopods indicates that stressing environmental factors were not low temperature or low salinity. Lower foraminiferal and algal diversity in the Khuff Formation may thus be chiefly ascribed to deposition in an epi-continental embayment, at a distance from the main Tethyan margin affected by the southern equatorial current and stressed by high fluviatile terrigenous influx documented by the significant siliciclastic fraction, resulting in an impoverished fusulinid and algal assemblage. This is supported by the fact that, moving southeastward along the Gonwanan margin to the Salt Range, the coeval Amb Formation shows a low-diversity fusulinid fauna – besides a rich brachiopod and bryozoan assemblage – related to a strong terrigenous imput and to high-energy settings (Mertmann, 1999).

5.2. Petrographic evidence for climatic change

Sandstones of the Haushi–Huqf document a marked increase in mineralogic stability from the Lower to the Middle Permian. Volcanic arenites in the Al Khlata Formation at Jabal Gharif and two-feldspar arkoses in the Saiwan Formation (Q 54–65; F 30–42, P/F 30–55; L 2–5; Angiolini et al., in press), pass upward to arkoses and subarkoses in the Gharif Formation (Q 57–86; F 14–40, P/F $\leq$ 44; L 0–3), and finally to quartz-rich K-feldspar subarkoses in the Khuff Formation (Fig. 6). Such a distinct trend suggests that selective destruction of labile components, prior to or after deposition, became progressively more effective with time.

Pre- and post-depositional alteration may produce similar features in thin sections, and assessing their relative incidence is a difficult task. Evidence for diagenetic dissolution can be generally detected, but pre-depositional weathering can seldom be demonstrated unambiguously, because of invariably superimposed diagenetic effects.

In the present case, diagenesis represents the most likely explanation for detrital-mode variability within each single Permian unit. However, very clear petrographic trends throughout the Permian indicate that the principal controlling factor is time-dependent, and other than diagenesis. Stratigraphically controlled diagenetic trends are in fact expected, other factors being equal, to cause removal of unstable components in older, not younger, strata. Good correlation with stratigraphic position (correlation coefficient 0.69–0.87, 0.1% significance level) suggests that half to three-fourths of the variance in detrital modes can be ascribed to such a time-dependent factor. Most significant is that the increase in quartz at the expense of all other components in younger beds is clearly associated with decreasing P/F ratio (correlation coefficient −0.88), documenting marked, selective plagioclase depletion in quartzose 'residual' sediments.

The relative abundances of plagioclase, orthoclase–perthite, and microcline in plutonic rocks are approximately 53/31/16 (Feniak, 1944, in Blatt, 1967). In unaltered plutoniclastic detritus, plagioclase is therefore expected to be equally or more abundant than K-feldspars, with orthoclase about twice as abundant as microcline. Chemical stability at low temperatures follows the opposite

order: microcline, with highly ordered structure, is more stable than orthoclase, and both are more stable than plagioclase. Preferential alteration of calcium-bearing plagioclase with respect to potassium feldspar, as documented by numerous works on recent soil profiles (e.g. Schroeder et al., 1997; Taboada and Garcia, 1999; Le Pera et al., 2001a), ensues from lower silicon–oxygen ratios, and hence fewer silicon–oxygen bonds. Sandstone suites characterized by P/F ratios <50 and microcline/KF ratios >33 may thus be suspected of having undergone preferential destruction of unstable feldspar grains.

In the Al Khlata to Saiwan formations, when cold to cool climates during and shortly after the Gondwanan glaciation are not likely to have fostered strong chemical weathering, P/F ratios range from 30 to 55, and cross-hatched microcline is locally as abundant as orthoclase, pointing to selective intrastratal solution of plagioclase (and even of orthoclase) in several samples. Plagioclase is moderately to very strongly altered, and both relatively fresh muscovite and altered biotite flakes commonly occur.

In the Gharif Formation, plagioclase grains are rarer, invariably strongly altered, and locally preserved only as ghosts. The P/F values decrease sharply to <25, and range up to 44 only if phyllosilicate patches are interpreted and re-apportioned as altered plagioclase. Twinned microcline represents $\leq 1/3$ of detrital K-feldspars, and locally shows intense alteration. Relatively fresh muscovite may be common. Altered biotite and epidote are rarely recorded.

In the Khuff Formation, altered plagioclase occurs only locally, being absent in most samples. Twinned microcline represents $\geq 1/3$ of detrital K-feldspars, indicating systematic enrichment with respect to orthoclase. Biotite is absent.

All of these features compare very well with theoretical weathering trends (Fig. 6; Nesbitt et al., 1997), confirming that sandstone petrography is controlled by chemical alteration of parent rocks and pedogenesis (Nesbitt et al., 1996; Le Pera et al., 2001b). Plagioclase clearly results by far as the most unstable grain type, followed by felsitic lithic grains, by orthoclase, and by microcline (Fig. 7). The observed stability series are: plagioclase → felsitic lithics → K-feldspar → microcline → quartz, and biotite → muscovite, fully consistent with the results of previous workers (e.g. Blatt, 1967).

With reference to quartz, assumed as not destroyed by either sedimentary or diagenetic processes, simple 'best fit' calculations show that when plagioclase is reduced to one-third of its original content, about half of felsitic grains and two-thirds of K-feldspars are still preserved. When plagioclase is weathered out, felsitic grains are reduced approximately to one-tenth, orthoclase to one-fourth, and microcline to half of their original contents.

The marked, long-term enrichment of chemically stable components in Permian sandstones is chiefly ascribed to more intense chemical weathering with time, fostered by progressively warmer and humid climates after the end of the Gondwanan glaciation and onset of spreading in the Neotethys Ocean. Development of more mature soil profiles was also favored by relative tectonic quiescence and reduced relief after the end of rifting, with consequently longer transit times of detritus from source to basin. Waning supply from the drowned shoulders of the rift, and increasing contribution from distant cratonic sources probably represented an additional cause for high quartz content in the Khuff Formation. Such contributions remain unconstrained.

It is impossible to assess precisely the relative incidence of shifting climates and possible provenance changes, which played out simoultaneusly. In our interpretation (Section 5.5) we stress the regional significance of climate change, which certainly did not involve only Interior Oman but most of northern Gondwana also. Alteration and pedogenesis are thus thought to be more active with time over a wide Arabian area, including all possible sources of Khuff detritus. Although several problems remain open, we present this case as one of the best ancient examples documenting the influence of chemical weathering on bulk composition.

5.3. Paleotectonic evolution

The Khuff Formation of Interior Arabia and

the correlative Saiq Formation of the North Oman Mountains are interpreted to reflect a major tectono-eustatic event, related to the onset of rapid thermal subsidence of the newly formed Arabian margin of Neotethys and drowning of the rift shoulders. This event has been interpreted as coeval with initiation of sea-floor spreading in the Neotethys Ocean by most authors (e.g. Bechennec et al., 1990; Blendinger et al., 1990, 1992; Stampfli et al., 1991; Pillevuit, 1993; Le Métour et al., 1994; Loosveld et al., 1996; Glennie, 2000; Sharland et al., 2001), who thus favored a Middle Permian opening.

Many interpretations of a Middle Permian break-up rely on the occurrence of pelagic limestones reported to contain Wordian ammonoids on top of basalts in the Oman Mountains (Blendinger et al., 1990). However, on the one hand the age of these well-known limestones – which are probably condensed – is still being debated, on the other, if these basalts are enriched MORB or alkaline (Maury et al., 2000), they can be interpreted in various ways (for instance, they might have been deposited on top of seamounts within Neotethys) and in neither case they contradict an Early Permian onset of Neotethyan spreading.

However, recent stratigraphic and petrographic data both on the Himalayan arm of Neotethys (Garzanti et al., 1994, 1996b, 1999) and on the failed Madagascar arm (Al-Belushi et al., 1996; Angiolini et al., in press) suggested that sea-floor spreading may have begun significantly earlier, around late Sakmarian times (Fig. 8). Break-up was followed by a proto-oeanic, Gulf-of-Aden-type stage, when heat flow remained high and the rift shoulders stood elevated in the absence of any significant thermal subsidence. The drowning of the main rift shoulder, possibly associated with faster sea-floor spreading and full oceanization, was delayed until Wordian times, some 18 Myr later. This is a reasonable minimum time gap, if the actualistic Gulf of Aden rift system is taken for comparison (e.g. Menzies et al., 1997). The rift shoulder of the Gulf of Aden today still reaches elevations close to 2000 m from Hadhramaut to Dhofar after up to 20 Myr of spreading along the Sheba Ridge (Platel and Roger, 1989), and much more time will elapse before Arabian Sea waters will be able to encroach onto the southern Arabian craton.

Drowning of the rift shoulders is very clearly documented in the Oman Mountains by shallow-

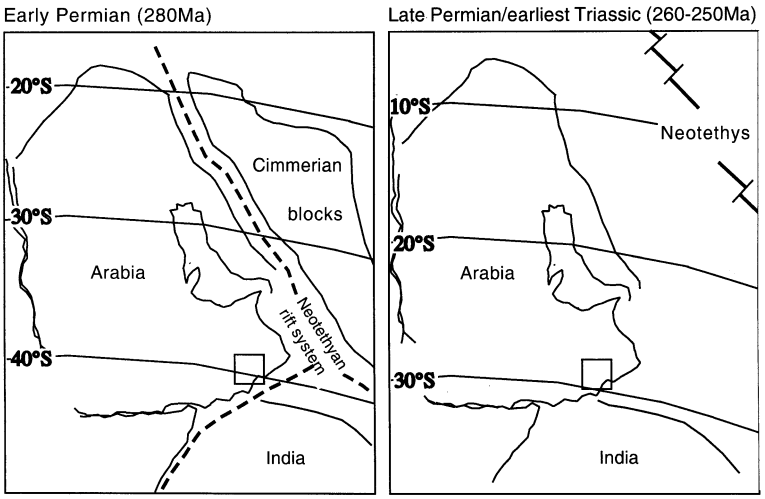

Fig. 8. Arabia paleogeography at Early Permian and Late Permian/earliest Triassic times with location of study area (empty square). Elements of Gondwana have been rotated relative to Arabia according to the parameters of Lottes and Rowley (1990), and oriented with respect to lines of paleolatitude with paleomagnetic poles of Muttoni et al. (1996) in Arabia coordinates. Neotethys opening and separation of the Cimmerian blocks from northern Gondwana is inferred to have begun around late Sakmarian times.

marine bioclastic limestones and dolostones of the Saiq Formation, overlying with marked angular unconformity various Upper Proterozoic carbonates to volcaniclastic units of the Jabal Akhdar dome (Bechennec et al., 1993). Our conodont data suggest a Wordian age for the base of the Saiq Formation at Wadi Sahtan, with the occurrence of *Hindeodus wordensis* at about 20 m from the base of the formation. We interpret such a sharp drowning event as the onset of thermal subsidence related to final displacement of the Neotethyan spreading axis far from the margin.

At Wordian times, Neotethyan sea-waters encroached onto a large portion of the Arabian platform, as documented by the Khuff Formation, with maximum flooding in the Haushi region being recorded by the sharp transition from Member 1 to Member 2. Recent Wordian paleogeographic reconstructions (Al-Aswad, 1997, p. 319; Gaetani et al., 2001) show a wide inner shelf covering most of Saudi Arabia, with outer-shelf settings in the southeast (Oman). A shelf margin with coral–algal build-ups (Weidlich, 1999), passing to slope and basinal deposits, is well documented in the Hawasina units exposed in the Oman Mountains (Pillevuit, 1993). Facies evolution from the Gharif to Khuff formations suggests that a wide embayment bordered the Interior Oman basin, with the southeastern coastline oriented roughly parallel to the Haushi–Huqf uplift, as indicated by sedimentary structures. The fact that subsidence now involves not only the rifted margins, but also large portions of Arabia, is consistent with transition from focused tectonic-related subsidence to widespread thermal subsidence (Busby and Ingersol, 1995).

Transgressive trends during Wordian times are recorded all along the northern Gondwana margin, from the Himalayas to Adria and Tunisia, and even in the Peri-Gondwanan fringe (Gaetani et al., 2001) to the Salt Range (Mertmann, 1999), documenting a turning point in the evolution of both successful and failed arms of the Tethyan rift system. There is no evidence for a gradual onlap, but for a sharp Wordian transgression in the Peri-Gondwanan regions, which we interpret as related to the onset of thermal subsidence of newly formed continental margins at the end of the proto-oceanic stage.

Thermal subsidence of the Interior Oman rim basin ceased soon after deposition of the Khuff Formation, capped disconformably by mature pedogenic profiles, whereas subsidence of passive margins facing both the Hawasina and Batain basins continued well into the Mesozoic (Watts and Garrison, 1986; Bechennec et al., 1990; Immenhauser et al., 1998).

5.4. Paleobiogeographic change

Statistic analyses comparing the Saiwan and the transitional Khuff brachiopod faunas with coeval faunas along the Peri-Gondwanan fringe (Central Afghanistan to South Thailand; Angiolini, 2001) reveal the dynamic nature of the provincial patterns during the Permian and a significant change of marine bioprovinciality from Sakmarian to Wordian times.

During the late Sakmarian, the Westralian Province extended all along the Peri-Gondwanan fringe, in response to raised humidity and lowering of temperature gradients immediately after the waning of the Gondwanan ice cap. At this stage, a strong link between Central Afghanistan and Interior Oman is evident, whereas a gradual eastward variation in the distribution of brachiopod genera is observed from Karakorum to Peninsular India and South Thailand, in response to the paleolatitudinal gradient.

At the beginning of the Middle Permian (Roadian–Wordian) two different provinces are developed south and north of the Neotethys Ocean: the Sibumasu Province – comprising Oman, Salt Range, and South Thailand – and the Transhimalayan Province, embracing Central Afghanistan and Karakorum. The Sibumasu Province is characterized by the generic association *Perigeyerella*, *Tornquistia*, *Celebetes*, *Bilotina*, *Haydenella*, *Stereochia*, *Cleiothyridina*, *Martiniopsis*, *Callispirina*, *Spiriferellina*, *Orbicoelia*, *Notothyris*, and *Hemyptichina*. Its temporal extension along the Gondwanan margin (Oman, Salt Range, Himalaya) is limited to the Middle Permian, and it probably overlaps with the Himalayan Province as amended by Shen and Shi (2000). However, the

Himalayan Province asserts itself and differentiates from the late Middle Permian onward. The Transhimalayan Province, extending from the end of the Early Permian along the Cimmerian continents, is identified by the generic association *Orthothetina*, *Sommeriella*, *Liraplecta* [= *Callytharrella* in Angiolini (1996)], *Compressoproductus*, *Septoconcha*, *Gruntoconcha*, *Reticulatia*. The increased proportion of paleoequatorial genera in the Transhimalayan Province indicates its northern and peripheral position with respect to the Sibumasu one.

The strong faunal link between South Oman and Central Afghanistan, clearly documented at Sakmarian times, abruptly ended before the end of the epoch. In fact, Middle Permian faunas in Central Afghanistan show only loose relationships with those of Oman and Salt Range, but are strongly connected to the Karakorum faunas. This major change in marine bioprovinciality supports the initial opening of the Neotethys before the Middle Permian, with the creation of a sufficiently large oceanic space to prevent biotic interchanges between the Gondwanan margin and the Cimmerian continents, resulting in disjunct distribution of fossil biota.

The distribution of marine bioprovinces during the Middle Permian is consistent with a surface ocean-circulation pattern as proposed by Archbold (1998, Fig. 7), with deflection of the southern paleoequatorial current to flow southeastward along the Gondwanan margin. This is also supported by the paleobiogeographic relationships of Khuff ostracodes, which may have been carried on floating algae by paleoequatorial surface currents from the western coast of Pangea to South China, Oman, Tunisia and Greece (Crasquin-Soleau et al., 2001).

5.5. Paleoclimatic interpretation

Independent evidence provided by sedimentologic, petrographic, paleontologic and paleomagnetic data suggests that Oman as part of the northern Gondwana margin moved progressively northward during the Middle Permian. Calculated paleolatitudes for the Haushi–Huqf (Lottes and Rowley, 1990; Muttoni et al., 1996) vary in fact from ca. 40°S during Sakmarian times to about 30°S during the Wordian (Fig. 8). Such a northward latitudinal shift towards the Southern Tropic is consistent with warmer temperatures suggested by paleontologic and petrographic indicators.

Warm and humid conditions documented in the Gharif and Khuff formations are compatible with the present-day climate of the east-facing coasts of the southern hemisphere continents at corresponding latitudes (i.e. southern Brasil, eastern South Africa), characterized by warm temperatures and sufficient precipitation all year round. Widening of Neotethys north of Oman, and drowning of the rift shoulders, may have forced the warm paleoequatorial current to be deflected southeastward along the northern Gondwanan margin, possibly exposed to southeasterly paleotrade winds. This pattern fits with the oceanic and atmospheric circulation pattern currently observed along the eastern coast of South America between 20 and 40°S and of Africa between 23 and 30°S.

Climatic changes inferred from paleontologic and petrographic indicators in Interior Oman can thus be largely ascribed to the documented northward latitudinal shift.

However, other factors may be considered, including the 'global-warming model' favored by several authors to have occurred from the Early Permian onward. For istance, according to Dickins (1993, 1996), bioprovincialism, oxygen isotopic curves, and worldwide distribution of glendonites, kaolin, and bauxite are all consistent with overall warming of Earth's climate after the Asselian and throughout the Permian, with a cold fluctuation in the mid-Permian. Wopfner (1999, 2001) has stressed the nearly simultaneous disappearance of glaciers all over Gondwana in the late Asselian to early Sakmarian, followed by deposition of coal measures in Madagascar, Tanzania, South Africa, and Antarctica, and by establishment of a seasonal warm to hot climate in south and central Africa during the Middle–Late Permian.

Global climatic warming, and consequent increase in precipitation rates, may thus explain high humidity inferred for Interior Oman at a latitude of about 30°S in the Middle Permian.

6. Conclusions

The Khuff Formation of Interior Arabia and the correlative Saiq Formation of North Oman document a major transgressive event of Wordian age, when Neotethyan waters encroached along vast portions of stable Arabia. Final drowning of the rift shoulders is ascribed to the onset of rapid thermal subsidence along the newly formed Arabian margin of Neotethys, about 18 Myr after continental break-up and initial separation between Gondwana and the Cimmerian blocks.

Composition of quartz-rich K-feldspar subarkoses in the Khuff Formation is fully consistent with a scenario of tectonic quiescence, progressively reduced topographic relief, and peneplanation of rift highlands in an advanced post-rift stage. The long-term enrichment of chemically stable detrital components during the Permian testifies to more intense chemical weathering with time, fostered by progressively warmer and humid climates after the end of the Gondwanan glaciation and onset of Neotethyan spreading.

The transitional character of the Khuff biota can be explained with the occurrence of an oceanic space in front of the Interior Oman basin, with free migration enhanced by warm surface currents along the Gondwanan margin and contemporaneous increase of biotic dissimilarity with the Cimmerian continents located on the northern margin of Neotethys.

The Permian faunal and petrographic evolution of the Interior Oman succession records a significant climatic change from glacial to warm and humid climates in about 25 Myr. Such a climate shift is related to the northward drift of Pangea at a plate speed of 4–10 cm/yr (Muttoni et al., 2001), to progressive opening of Neotethys to the north, and to warming of Earth climates after the earliest Permian.

Acknowledgements

Hilal Al-Azri and Harub Al-Hashmi of the Directorate General of Minerals (Muscat) are thanked for logistic assistence. J. Roger, J.P. Platel, J. Broutin, A. Baud, J. Marcoux, H. Bucher are warmly thanked for field assistance. Benoit Beauchamp and Gerard Stampfli are warmly thanked for detailed and constructive revision. Giovanni Chiodi, Curzio Malinverno and Gabriele Pezzi are thanked for technical assistance. Gigi Battagion and Giovanni Vezzoli gave precious help in petrographic analysis of sandstone samples.

References

Al-Aswad, A.A., 1997. Stratigraphy, sedimentary environment and depositional evolution of the Khuff Formation in south-central Saudi Arabia. J. Petrol. Geol. 20, 307–326.

Al-Belushi, J., Glennie, K.W., Williams, B.P.J., 1996. Permo-Carboniferous glaciogenic Al Khlata Formation, Oman: A new hypothesis for origin of its glaciation. GeoArabia 1, 389–403.

Angiolini, L., 1996. Permian brachiopods from Karakorum. Pt. 2. Riv. Ital. Paleontol. Stratigr. 102, 3–26.

Angiolini, L., 2001. Middle Permian brachiopods from Oman and Peri-Gondwanan palaeogeographic reconstructions. In: Brunton, C.H.C., Cocks, L.R.M., Long, S.L. (Eds.), Brachiopods Past and Present. The Systematic Association Special Volume Series 63, pp. 352–362.

Angiolini, L., Bucher, H., 1999. Guadalupian brachiopods from the Khuff Formation, southeastern Oman. Geobios 32, 665–699.

Angiolini, L., Balini, M., Garzanti, E., Nicora, A., Tintori, A. Gondwanan deglaciation and opening of Neotethys: the Al-Khlata and Saiwan Formations of Interior Oman. Palaeogeogr. Palaeoclimatol. Palaeoecol., in press.

Angiolini, L., Bucher, H., Pillevuit, A., Platel, J.P., Roger, J., Broutin, J., Baud, A., Marcoux, J., Al-Hashmi, H., 1997. Early Permian (Sakmarian) brachiopods from south-eastern Oman. Geobios 30, 389–406.

Angiolini, L., Nicora, A., Bucher, H., Vachard, D., Pillevuit, A., Platel, J.P., Roger, J., Baud, A., Broutin, J., Al-Hashmi, H., Marcoux, J., 1998. Evidence of a Guadalupian age for Khuff Formation of South-eastern Oman: preliminary report. Riv. Ital. Paleontol. Stratigr. 104, 329–340.

Archbold, N.W., 1998. Correlations of the western Australian Permian and Permian ocean circulation patterns. Proc. R. Soc. Vic. 110, 85–106.

Archbold, N.W., Shi, G.R., 1995. Permian brachiopod faunas of Western Australia: Gondwanan-Asian relationships and Permian climate. J. Southeast Asian Earth Sci. 11, 207–215.

Bechennec, F., Le Métour, J., Platel, J.P., Roger, J., 1993. Geological map of the Sultanate of Oman, scale 1:1.000.000 and explanatory notes. Directorate General of Minerals, Oman Ministry of Petroleum and Minerals.

Bechennec, F., Le Métour, J., Rabu, D., Bourdillon-Jeudy de Grissac, C., De Wever, P., Beurrier, M., Villey, M., 1990. The Hawasina Nappes: stratigraphy, palaeogeography and

structural evolution of a fragment of the South Tethyan passive continental margin. In: Robertson, A.H., Searle, M.P., Ries, A.C. (Eds.), The Geology and Tectonics of the Oman Region. Geological Society of London Special Publication 49, pp. 213–223.

Bender, H., Stoppel, D., 1965. Perm-Conodonten. Geol. Jahrb. 82, 331–364.

Blatt, H., 1967. Provenance determinations and recycling of sediments. J. Sediment. Petrol. 37, 1031–1044.

Blendinger, W., Van Vliet, A., Hughes-Clarke, M.W., 1990. Updoming, rifting and continental margin development during the Late paleozoic in Northern Oman. In: Robertson, A.H., Searle, M.P., Ries, A.C. (Eds.), The Geology and Tectonics of the Oman Region. Geological Society of London Special Publication 49, pp. 27–37.

Blendinger, W., Furnish, W.M., Glenister, B.F., 1992. Permian cephalopods limestones, Oman Mountains: evidence for a Permian sea-way along the northern margin of Gondwana. Palaeogeogr. Palaeoclimatol. Palaeoecol. 93, 13–20.

Broutin, J., Roger, J., Platel, J.P., Angiolini, L., Baud, A., Bucher, H., Marcoux, J., Al-Hashmi, H., 1995. The Permian Pangea. Phytogeographic implications of new palaeontological discoveries in Oman (Arabian Peninsula). C.R. Acad. Sci. Paris 321, 1069–1086.

Busby, C.J., Ingersol, R.V., 1995. Tectonics of Sedimentary Basins. Blackwell, Oxford, 579 pp.

Cleary, W.J., Conolly, J.R., 1972. Embayed quartz grains in soils and their significance. J. Sediment. Petrol. 42, 899–904.

Coryell, H.N., Sample, C.H., 1932. Pennsylvanian Ostracoda. A study of the Ostracoda fauna of the East Mountain Shale, Mineral Wells Formation. Am. Midl. Nat. 13, 245–281.

Costenzo, G.V., Kaesler, R.L., 1987. Changes in Permian marine ostracode fauna during regression, Florena shale, northeastern Kansas. J. Paleontol. 61, 1204–1215.

Crasquin-Soleau, S., Broutin, J., Besse, J., Berthelin, M., 2001. Ostracodes and palaeobotany from the Middle Permian of Oman: implications on Pangaea reconstruction. Terra Nova 13, 38–43.

Crasquin-Soleau, S., Broutin, J., Roger, J., Platel, J.P., Al-Hashmi, H., Angiolini, L., Baud, A., Bucher, H., Marcoux, J., 1999. First Permian ostracode fauna from the Arabian Plate (Khuff Formation, Sultanate of Oman). Micropalaeontology 45, 163–182.

Crumeyrolle, P., Razin, P., Roger, J., Platel, J.P., 1997. Sedimentology, sequence stratigraphy and reservoir geometry of the upper Gharif and lower Khuff Formations, Permian of Oman, Haushi outcrop study. TOTAL/BRGM Report 2536.

Dickins, J.M., 1993. Climate of the Late Devonian to Triassic. Palaeogeogr. Palaeoclimatol. Palaeoecol. 100, 89–94.

Dickins, J.M., 1996. Problems of a Late Palaeozoic glaciation in Australia and subsequent climate in the Permian. Palaeogeogr. Palaeoclimatol. Palaeoecol. 125, 185–197.

Dickins, J.M., 1999. Mid-Permian (Kubergandian–Murgabian) bivalves from the Khuff Formation, Oman: implications for world events and correlations. Riv. Ital. Paleontol. Stratigr. 105, 23–35.

Dickinson, W.R., 1970. Interpreting detrital modes of graywacke and arkose. J. Sediment. Petrol. 40, 695–707.

Dickinson, W.R., 1985. Interpreting provenance relations from detrital modes of sandstones. In: Zuffa, G.G. (Ed.), Provenance of Arenites. Reidel, Dordrecht, pp. 333–361.

Dubreuilh, J., Béchennec, F., Berthiaux, A., Le Métour, J., Platel, J.P., Roger, J., Wyns, R., 1992. Geological map of Khaluf, Sheet NF40-15, scale 1:250,000 and explanatory notes. Directorate General of Minerals, Oman Ministry of Petroleum and Minerals.

Dutta, P.K., 1992. Climatic influence on diagenesis of fluvial sandstones. In: Wolf, K.H., Chilingarian, G.V. (Eds.), Diagenesis III, Developments in Sedimentology 47, pp. 191–251.

Epstein, A.G., Epstein, J.B., Harris, L.D., 1977. Conodont color alteration - an index to organic metamorphism. Geol. Surv. Prof. Paper 995, 1–27.

Fluteau, F., Besse, J., Broutin, J., Berthelin, M., 2001. Extension of Cathaysian flora during the Permian. Climatic and paleogeographic constraints. Earth Planet. Sci. Lett. 193, 603–616.

Gaetani, M., Arche, A., Kiersnowski, H., Chuvachov, B., Crasquin, S., Sandulescu, M., Seghedi, A., Zagorchev, I., Poisson, A., Hirsch, F., Vaslet, D., Le Métour, J., Ziegler, M., Abbate, E., Ait-Brahim, L., Barrier, E. Bouaziz, S., Bergerat, F., Brunet, M.F., Cadet, J.P., Stephenson, R., Guezou, J.C., Jabaloy, A., Lepvrier, C., Rimmele, G., 2001. Wordian paleogeographic map. In: Dercourt, J., Gaetani, M., et al. (Eds.), Peri-Tethys Atlas and Explanatory Notes, map 3, GM/CGMW, Paris, pp. 19–25.

Garzanti, E., Sciunnach, D., 1997. Early Carboniferous onset of Gondwanian glaciation and Neo-Tethyan rifting in Southern Tibet. Earth Planet. Sci. Lett. 148, 359–365.

Garzanti, E., Angiolini, L., Sciunnach, D., 1996a. The mid-Carboniferous to lowermost Permian succession of Spiti (Po Group and Ganmachidam Formation; Tethys Himalaya, Northern India): Gondwana glaciation and rifting of Neo-Tethys. Geodin. Acta 9, 78–100.

Garzanti, E., Angiolini, L., Sciunnach, D., 1996b. The Permian Kuling Group (Spiti, Lahaul and Zanskar; NW Himalaya): sedimentary evolution during rift/drift transition and initial opening of Neo-Tethys. Riv. Ital. Paleontol. Stratigr. 102, 175–200.

Garzanti, E., Le Fort, P., Sciunnach, D., 1999. First report of Lower Permian basalts in South Tibet: tholeiitic magmatism during break-up and incipient spreading in Neo-tethys. J. Asian Earth Sci. 17, 533–546.

Garzanti, E., Vezzoli, G., Andò, S., Castiglioni, G., 2001. Petrology of rifted-margin sand (Red Sea and Gulf of Aden, Yemen). J. Geol. 109, 277–297.

Garzanti, E., Nicora, A., Tintori, A., Sciunnach, D., Angiolini, L., 1994. Late Paleozoic stratigraphy and petrography of the Thini Chu Group (Manang, Central Nepal): sedimentary record of Gondwana glaciation and rifting of Neotethys. Riv. Ital. Paleontol. Stratigr. 100, 155–194.

Girty, G.H., 1909. The Guadalupian fauna. United States Geological Survey Professional Paper 58, 651 pp.

Glennie, K.W., 2000. Cretaceous tectonic evolution of Ara-

bia's Eastern Plate margine: A tale of two oceans. SEPM Spec. Publ. 69, 9–20.
Grant, R.E., 1976. Permian brachiopods from southern Thailand. J. Paleontol. 50, suppl. to 3, Paleontological Society Memoirs 9, 254 pp.
Guex, J., 1991. Biochronological Correlations. Springer, 250 pp.
Hagdorn, H., Mundlos, R., 1983. Aspekte der Taphonomie von Muschelkalk-Cephalopoden Teil 1: Siphozerfall und Füllmechanismus. N. Jb. Geol. Paläont. Abh. 166, 369–403.
Hudson, R.G.S., Sudbury, M., 1959. Permian brachiopoda from south-east Arabia. Notes Mém. Moyen-Orient Muséum Nat. d'Histoire Naturelle Paris 7, 19–55.
Immenhauser, A., Schreurs, G., Peters, T., Matter, A., Hauser, M., Dumitrica, P., 1998. Stratigraphy, sedimentology and depositional environments of the Permian to uppermost Cretaceous Batain Group, eastern-Oman. Eclogae Geol. Helv. 91, 217–235.
Jin, Y., Wardlaw, B.R., Glenister, B.F., Kotlyar, G.V., 1997. Permian chronostratigraphy subdivisions. Episodes 20, 10–15.
Johnsson, M.J., 1993. The system controlling the composition of clastic sediments. In: Johnsson, M.J., Basu, A. (Eds.), Processes Controlling the Composition of Clastic Sediments. Geological Society of America Special Paper 284, pp. 1–19.
Kotlyar, G.V., Pronina, G.P., 1995. Murgabian and Midian Stages of the Tethyan realm. Permophiles 27, 23–26.
Kozur, H., 1995. Permian conodont zonation and its importance for the Permian stratigraphic standard scale. Geol. Palaeontol. Mitt. Innsbruck 20, 165–205.
Kozur, H., Mostler, H., 1976. Neue Conodonten aus dem Jungpalaozoikum und der Trias. Geol. Palaeontol. Mitt. Innsbruck 6, 1–33.
Le Métour, J., Béchennec, F., Platel, J.P., Roger, J., 1994. Late Permian birth of the Neo-Tethys and development of its Southern continental margin in Oman. The Middle East Petroleum Geosciences – Selected Middle East papers from the Middle East Geosciences Conference, Bahrain, April 1994, vol. 2, pp. 643–654.
Le Pera, E., Arribas, J., Critelli, S., Tortosa, A., 2001a. The effects of source rocks and chemical weathering on the petrogenesis of siliciclastic sand from the Neto River (Calabria, Italy): implications for provenance studies. Sedimentology 48, 357–378.
Le Pera, E., Critelli, S., Sorriso-Valvo, M., 2001b. Weathering of gneiss in Calabria, Southern Italy. Catena 42, 1–15.
Lethiers, F., Crasquin-Soleau, S., 1988. Comment extraire des microfossiles à tests calcitiques de roches calcaires dures. Rev. Micropaléontol. 31, 56–61.
Levell, B.K., Braakman, J.H., Rutten, K.W., 1988. Oil-bearing sediments of Gondwana glaciation in Oman. Am. Assoc. Pet. Geol. Bull. 72, 775–796.
Loosveld, R.J.H., Bell, A., Terken, J.J.M., 1996. The tectonic evolution of Interior Oman. GeoArabia 1, 28–51.
Lottes, A.L., Rowley, D.B., 1990. Reconstruction of the Laurasian and Gondwanan segments of Permian Pangaea. In: McKerrow, W.S., Scotese, C.R. (Eds.), Palaeozoic Palaeogeography and Biogeography. Geological Society Memoir 12, pp. 383–395.
Maury, R.C., Cotten, J., Bechennec, F., Caroff, M., Marcoux, J., 2000. Magmatic evolution of the Tethyan Permo-Triassic Oman margin. International Conference Geology of Oman, Muscat, January 12–16 2001, Abstracts, p. 60.
McBride, E.F., 1985. Diagenetic processes that affect provenance determinations in sandstones. In: Zuffa, G.G. (Ed.), Provenance of Arenites. NATO-ASI Series 148, Reidel, Dordrecht, pp. 95–113.
Melnyk, D.H., Maddocks, R.F., 1988. Ostracodee biostratigraphy of the Permo-Carboniferous of Central and North-Central Texas, part I: Paleoenvironmental framework. Micropaleontology 34, 1–20.
Menzies, M., Gallagher, K., Yelland, A., Hurford, A.J., 1997. Volcanic and nonvolcanic rifted margins of the Red Sea and Gulf of Aden: crustal cooling and margin evolution in Yemen. Geochim. Cosmochim. Acta 61, 2511–2527.
Mertmann, D., 1999. Die Faziesentwicklung der Zaluch-Gruppe (Perm) in der Salt Rangenund in den Trans Indus Range, Pakistan. Berliner Geowissenschaftliche Abhandlungen A 204, 94 pp.
Miller, A.K., Furnish, W.N., 1957. Permian ammonoids from Southern Arabia. J. Palaeontol. 31, 1043–1051.
Muttoni, G., Kent, D.V., Channell, J.E.T., 1996. The evolution of Pangea: Paleomagnetic constraints from the Southern Alps, Italy. Earth Planet. Sci. Lett. 140, 97–112.
Muttoni, G., Garzanti, E., Alfonsi, L., Cirilli, S., Germani, D., Lowrie, W., 2001. Motion of Africa and Adria since the Permian: Paleomagnetic and paleoclimatic constraints from northern Libya. Earth Planet. Sci. Lett. 92, 159–174.
Nesbitt, H.W., Young, G.M., McLennan, S.M., Keays, R.R., 1996. Effects of chemical weathering and sorting on the petrogenesis of siliciclastic sediments, with implications for provenance studies. J. Geol. 104, 525–542.
Nesbitt, H.W., Fedo, C.M., Young, G.M., 1997. Quartz and feldspar stability, steady and non-steady-state weathering, and petrogenesis of siliciclastic sands and muds. J. Geol. 105, 173–191.
Peterson, R.M., Kaesler, R.L., 1980. Distribution and diversity of ostracodee assemblages from the Hamlin shale and the Americcus limestone (Permian, Wolfcampian) in Northeastern Kansas. Univ. Kansas Paleontol. Contrib. 100, 1–26.
Pillevuit, A., 1993. Les Blocs Exotiques du Sultanat d'Oman. Evolution paleogeographique d'une marge passive flexurale. Memoires Geologie Lausanne 17, 249 pp.
Platel, J.P., Roger, J., 1989. Evolution géodinamique du Dhofar (Sultanat d' Oman) pendant le Crétacé et le Tertiaire en relation avec l' ouverture du golfe d' Aden. Bull. Soc. Géol. France 8, 253–263.
Reed, F.R.C., 1944. Brachiopods and Mollusca from the Productus Limestone of the Salt Range. Palaeontol. Indica N.S. 23, 1–678.
Rejebian, V.A., Harris, A.G., Huebner, J.S., 1987. Conodont color and textural alteration: An index to regional metamorphism, contact metamorphism, and hydrothermal alteration. Geol. Soc. Am. Bull. 99, 471–479.

Roger, J., Chevrel, S., Platel, J.P., Béchennec, F., Dubreuilh, J., Le Métour, J., Wyns, R., 1992. Geological map of Mafraq, Sheet NF 40-11, scale 1:250,000 and explanatory notes. Directorate General of Minerals, Oman Ministry of Petroleum and Minerals.

Schroeder, P.A., Kim, J.G., Melear, N.D., 1997. Mineralogical and textural criteria for recognizing remnant Cenozoic deposits on the Piedmont: evidence from Sparta and Greene County, Georgia, USA. Sediment. Geol. 108, 195–206.

Sharland, P.R., Archer, R., Casey, D.M., Davies, R.B., Hall, S.H., Heward, A.P., Horbury, A.D., Simmons, M.D., 2001. Arabian Plate Sequence Stratigraphy. GeoArabia Special Publication 2, 371 pp.

Shen, S., Shi, G.R., 2000. Wuchiapingian (early Lopingian, Permian) global brachiopod palaeobiogeography: a quantitative approach. Palaeogeogr. Palaeoclimatol. Palaeoecol. 162, 299–318.

Shi, G.R., Archbold, N.W., 1995. Palaeobiogeography of Kazanian-Midian (late Permian) western Pacific Brachiopod faunas. J. Southeast Asian Earth Sc. 12, 129–141.

Shi, G.R., Archbold, N.W., 1998. Permian marine biogeography of SE Asia. In: Hall, R., Holloway, J.D. (Eds.), Biogeography and Geological Evolution of SE Asia, Leiden, pp. 57–72.

Shi, G.R., Archbold, N.W., Zhan, L.P., 1995. Distribution and characteristics of mixed (transitional) mid-Permian (Late Artinskian-Ufimian) marine faunas in Asia and their palaeogeographical implications. Palaeogeogr. Palaeoclimatol. Palaeoecol. 114, 241–271.

Stampfli, G.M., 2000. Tethyan oceans. In: Bozkurt, E., Winchester, J.A., Piper, J.D.A. (Eds.), Tectonics and Magmatism in Turkey and the Sorrounding Area. Geological Society of London Special Publications 173, pp. 1–23.

Stampfli, G., Marcoux, J., Baud, A., 1991. Tethyan margins in space and time. Palaeogeogr. Palaeoclimatol. Palaeoecol. 87, 373–409.

Stehli, F.G., 1970. A test of the earth magnetic field during Permian time. J. Geophys. Res. 75, 3325–3342.

Steineke, M., Bramkamp, R., Sander, N.J., 1958. Stratigraphic relations of Arabian Jurassic oil. In: Weeks, L.G. (Ed.), Habitat of Oil. AAPG, Tulsa, OK, pp. 1294–1339.

Suttner, L.J., Dutta, P.K., 1986. Alluvial sandstone composition and paleoclimate. I. Framework mineralogy. J. Sediment. Petrol. 56, 329–345.

Swift, A., Aldrige, R.J., 1982. Conodonts from the Upper Permian strata of the Nottinghamshire and North Yorkshire. Palaeontology 25, 845–856.

Taboada, T., Garcia, C., 1999. Pseudomorphic transformation of plagioclases during weathering of granitic rocks in Galicia (NW Spain). Catena 35, 293–304.

Vannay, J.C., 1993. Géologie des chaines du Haut Himalaya et du Pir Panjal au Haut Lahul (NW-Himalaya, Inde). Mém. Géol. Lausanne 16, 1–148.

Waagen, W.H., 1882–1885. Salt range fossils. Part 4: Brachiopoda. Palaeontologia Indica 13, 329–770.

Wang, S.Q., 1978. Late Permian and Early Triassic ostracodes of western Guizhou and northeastern Yunnan (in Chinese). Acta Palaeontol. Sinica 17, 277–312.

Wardlaw, B.R., 1995. Permian conodonts. In: Scholle, P.A., Peryt, T.M., Ulmer-Scholle, D.S. (Eds.), The Permian of Northern Pangea. Springer, pp. 186–195.

Wardlaw, B.R., 2000. Guadalupian Conodont Biostrastigraphy of the Glass and Del Norte Mountains. In: Wardlaw, B.R., Grant, R.E., Rohr, D.M. (Eds.), Smithsonian Contributions to the Earth Sciences 32, pp. 37–87.

Wardlaw, B.R., Collinson, J.W., 1984. Conodont paleoecology of the Permian Phosphoria Formation and related rocks of Wyoming and adjacent areas. In: Clark, D.L. (Ed.), Conodont Biofacies and Provincialism. Geological Society of America Special Paper 196, pp. 263–281.

Wardlaw, B.R., Collinson, J.W., 1986. Paleontology and deposition of the Phosphoria Formation. Contrib. Geol. Univ. Wyoming 24, 107–142.

Wardlaw, B.R., Pogue, K.R., 1995. The Permian of Pakistan. In: Scholle, P.A., Peryt, T.M., Ulmer-Scholle, D.S. (Eds.), The Permian of Northern Pangea. Springer, pp. 215–224.

Watts, K.F., Garrison, R.E., 1986. Sumeini Group, Oman. Evolution of a Mesozoic carbonate slope on a South Tethyan continental margin. Sediment. Geol. 48, 107–168.

Weidlich, O., 1999. Taxonomy and reefbuilding potential of Middle/Late Permian Rugosa and Tabulata in platform and reef environments. N. Jahrb. Geol. Palaeontol. Abhandl. 211, 113–131.

Wopfner, H., 1999. The Early Permian deglaciation event between East Africa and northwestern Australia. J. Afr. Earth Sci. 29, 77–90.

Wopfner, H., 2001. Late Palaeozoic to Early Triassic climatic transition between Africa and the Southern Alps. International Conference Geology of Oman, Muscat, January 12–16, 2001, Abstracts, p. 89.